STIEFELD, ROBYN ERICA

THE CHARACTERIZATION OF THERMALLY GROWN TUNGSTEN OXIDE FORMATION ON THIN FILM TUNGSTEN

THE UNIVERSITY OF ARIZONA M.S. 1984

PLEASE NOTE:

In all cases this material has been filmed in the best possible way from the available copy. Problems encountered with this document have been identified here with a check mark __✓__.

1. Glossy photographs or pages _____
2. Colored illustrations, paper or print _____
3. Photographs with dark background _____
4. Illustrations are poor copy _____
5. Pages with black marks, not original copy _____
6. Print shows through as there is text on both sides of page _____
7. Indistinct, broken or small print on several pages __✓__
8. Print exceeds margin requirements _____
9. Tightly bound copy with print lost in spine _____
10. Computer printout pages with indistinct print _____
11. Page(s) _____ lacking when material received, and not available from school or author.
12. Page(s) _____ seem to be missing in numbering only as text follows.
13. Two pages numbered _____. Text follows.
14. Curling and wrinkled pages _____
15. Dissertation contains pages with print at a slant, filmed as received _____
16. Other _____

_____

_____

University
Microfilms
International

THE CHARACTERIZATION OF THERMALLY GROWN TUNGSTEN OXIDE FORMATION ON THIN FILM TUNGSTEN

by

Robyn E. Stiefeld

A Thesis Submitted to the Faculty of the

DEPARTMENT OF ELECTRICAL AND COMPUTER ENGINEERING

In Partial Fulfillment of the Requirements
For the Degree of

MASTER OF SCIENCE

In the Graduate College

THE UNIVERSITY OF ARIZONA

1 9 8 4

STATEMENT BY AUTHOR

This thesis has been submitted in partial fulfillment of requirements for an advanced degree at The University of Arizona and is deposited in the University Library to be made available to borrowers under rules of the Library.

Brief quotations from this thesis are allowable without special permission, provided that accurate acknowledgment of source is made. Requests for permission for extended quotation from or reproduction of this manuscript in whole or in part may be granted by the head of the major department or the Dean of the Graduate College when in his or her judgment the proposed use of the material is in the interests of scholarship. In all other instances, however, permission must be obtained from the author.

SIGNED: Robyn Erica Stiefeld

APPROVAL BY THESIS DIRECTOR

This thesis has been approved on the date shown below:

James N. Fordemwalt — 11-30-84

JAMES N. FORDEMWALT — Date

Professor of Electrical and Computer Engineering

DEDICATION

This thesis is dedicated to my mother and father, Kevin, and the rest of my family.

ACKNOWLEDGMENT

I would like to thank Mr. Len Raymond and Dr. James N. Fordemwalt at the University of Arizona for their contributions to this thesis. I would also like to thank Dr. Victor A. Wells at Sandia National Laboratories in Albuquerque, New Mexico, for his support and encouragement during the course of this project. Additionally, I would like to thank Dr. Wells' staff--Maren Tracy and Dr. Robert Blewer--for assisting me in getting materials and information.

Finally, I would like to thank Dr. John Leavitt at the University of Arizona for his time required to make Rutherford Backscattering measurements. I would like to thank Susan Kinsey for her part in typing this thesis.

TABLE OF CONTENTS

LIST OF ILLUSTRATIONS

LIST OF ILLUSTRATIONS--Continued

LIST OF TABLES

ABSTRACT

The oxidation of thin film tungsten was investigated in the temperature range from 300°C to 525°C using oxygen at one atmosphere. Tungsten samples came from two sources. The first source was a cold wall low pressure chemical vapor deposition process. The second source was a hot wall reduced pressure chemical vapor deposition process.

The characterization of the oxide film was done physically and optically. The properties of the oxide films that were investigated are: refractive index, growth rate, resistivity, and stoichiometry. Additionally, the passivation of the tungsten film was investigated. The passivating films used were silicon dioxide and silicon nitride.

CHAPTER 1

INTRODUCTION

During the course of the next few years, the degree of complexity of integrated circuit design and manufacturing will increase significantly. In order to accommodate the inherent problems that are associated with the changes from several microns to sub-micron geometry, manufacturing and design techniques will have to be optimized. This optimization will include both new manufacturing techniques as well as new materials to replace those currently being used. One such material is tungsten, which is being investigated for use in metalization processes. Tungsten could be used to replace aluminum as part of a multilevel metalization scheme.

There are several reasons why tungsten is being investigated for metalization. Tungsten has: (1) a high melting point which lends itself nicely to follow on processes in integrated circuit fabrication, (2) low resistivity, and (3) good adhesion to silicon and other materials used in fabrication. (4) The coefficient of expansion is similar to silicon. (5) Tungsten does not diffuse easily into silicon because of the high melting point of the tungsten-silicon system. (6) The deposition process for tungsten is similar to the processing currently being used in fabrication lines.

The bulk properties of tungsten include a melting point of 3300°C and resistivity of 5.8$\mu\Omega$/cm. One major problem that must be

considered when tungsten is used in fabrication is that it oxidizes at temperatures around 300°C (Shaw and Amick 1971). Because of this property, care must be taken to passivate tungsten prior to fabrication procedures done at elevated temperatures.

The objective of this thesis is to characterize thermally grown tungsten oxide on thin film tungsten. The temperatures investigated were between 300°C and 525°C using one atmosphere in oxygen. The thin film tungsten came from two sources. The first source was the University of Arizona (U of A). These samples were prepared by cold wall low pressure chemical vapor deposition (LPCVD). The second source was Sandia National Laboratories in Albuquerque, New Mexico (SNL). Their samples were prepared by hot wall reduced pressure chemical vapor deposition (RPCVD).

The physical properties that will be discussed are:

1. The oxide growth rate at various temperatures for both types of tungsten films.
2. The stoichiometry and uniformity of the oxide layer for both types of tungsten films.
3. The optical properties as a function of thickness--primarily the index of refraction.
4. The electrical properties--primarily resistivity for both types of films.
5. Passivation of tungsten using silicon dioxide and silicon nitride at elevated temperatures to see if oxidation occurs (for U of A samples only).

In order to investigate the physical properties of the tungsten oxide, a test mask was designed that could be used for general process characterization. The test mask contained:

1. A ten square Kelvin resistor with a width of 100μm.
2. A 524 square serpentine Kelvin resistor with a width of 25μm.
3. Kelvin resistors to measure contact resistance with contact window sizes of 25μm x 25μm and 10μm x 10μm.
4. MOS capacitors of three sizes with multiple electrodes--450μm x 250μm, 25μm x 25μm, and 10μm x 10μm.

Generally, both types of tungsten oxidized following a parabolic rate at temperatures of interest. Additionally, the U of A cold wall LPCVD tungsten appeared to oxidize at a faster rate at all temperatures than the SNL hot wall RPCVD samples. Both types of tungsten oxide films had resistivities in the range of 100Ω-cm to 1000Ω-cm depending on the oxide film thickness. The index of refraction appeared to be a function of thickness.

The remainder of this thesis addresses the above concerns as described by the following chapters.

Chapter 2. The general theory of oxidation and oxidation rate curves.

Chapter 3. Physical characterization along with method of analysis.

Chapter 4. Passivation of tungsten using silicon dioxide and silicon nitride.

Chapter 5. Summary

CHAPTER 2

OXIDATION OF THIN FILM TUNGSTEN

Tungsten has extremely favorable properties as a refractory metal with the exception of a low oxidation temperature of 300°C. During the course of integrated circuit fabrication, there are many processes that take place at higher temperatures. The oxidation of the thin film tungsten was investigated at temperatures between 300°C and 525°C in 75° increments. The oxidation of tungsten can take place by simply pulling tungsten hot (above 300°C) into standard ambient conditions. Therefore, some care was taken to control and standardize oxidation conditions. One factor that was not investigated was native oxide which is considered to be the oxide that forms in ambient conditions. This oxide is typically 10 to 50Å thick and forms a protective film on the tungsten. All tungsten samples were left at room temperature for some time prior to their use. It was assumed that this native oxide was present on all wafers and was not considered. The oxidation of tungsten at high temperature was also not considered because of the tungsten film thickness that would be required for oxidation, and because of temperature constraints of the furnace.

Two types of samples were prepared and oxidized for comparison. The first type of sample was prepared by the University of Arizona using a cold wall LPCVD process. The second type of sample was prepared by Sandia National Laboratories using hot wall reduced pressure CVD.

Figure 1 shows the film structure of the two types of prepared samples.

A matrix of times and temperatures was set up for testing procedures. The matrix consisted of times of 10, 50, and 90 minutes and temperatures of 300°C, 375°C, 450°C, and 525°C. For each point of the matrix, two pieces of each sample were oxidized. The first of the two pieces was not delineated; whereas, the second piece had a delineated pattern of test devices on it.

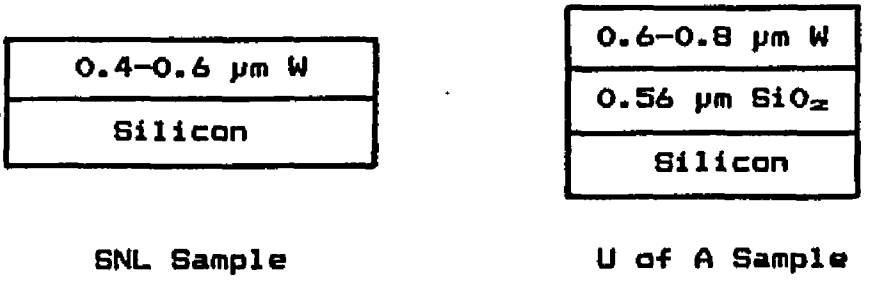

Figure 1. Film Structure of Tungsten Samples.

Prior to actual data collection, testing was completed to optimize the oxidation process. The process parameters that were investigated were gas flow, temperature uniformity, and wafer placement. The major criterion for optimization was the repeatability and uniformity of the oxide film based on color uniformity from run to run. The difference in non-color uniformity could not be quantitatively measured because of the inaccuracy in the Tencor Alpha Step in the range of interest, and the ellipsometer not being readily available.

Figure 2 shows the dimensions of the furnace that was used throughout the investigation. In addition, all oxidation processes took place with a cap in place on the quartz tube. This cap had a half inch diameter hole to allow a steady gas flow through the tube.

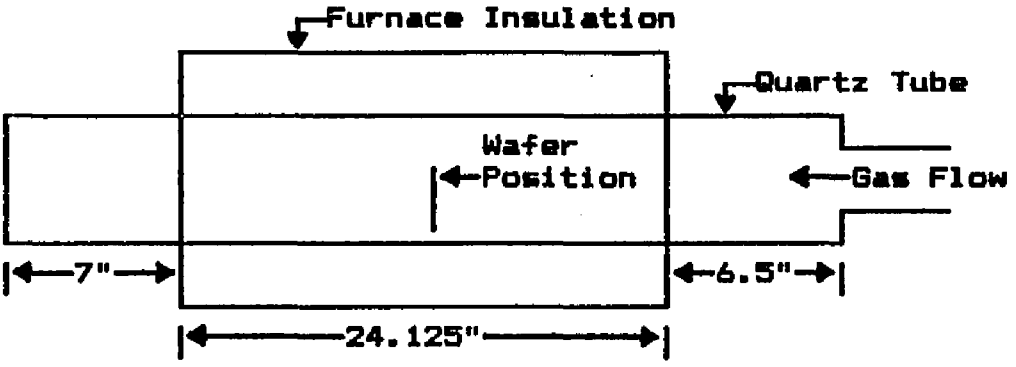

Figure 2. Furnace Structure.

The first parameter to be considered was oxygen gas flow. The gas flow was tested from 2.0 liters/min down to 0.3 liters/min. Two major factors were considered prior to the choice of an operating point. The first factor is the cooling of the wafer surface due to the gas flow. The second factor is gas depletion at the wafer surface. Using a R-2-15-D stainless steel ball Brooks flow meter at a flow rate of 0.475 liter/min gave the most repeatable results.

The next processing parameter that was looked at was the temperature profile of the furnace. The major concern is to have a uniform hot zone around the location of the wafers. Table 1 shows the uniformity of the temperature at 400°C, 450°C, and 500°C. The

Table 1. Furnace Temperature Profile

Position (Inches)	Temperature		
	400°C	450°C	500°C
+3.0	406	460	512
+2.0	408	460	512
+1.5	408	459	509
+1.0	407	457	507
+0.5	404	453	504
0.0	402	450	499
-0.5	402	446	493
-1.0	399	434	485
-1.5	395	426	476
-2.0	387	424	472

temperatures were profiled going in both directions (positive moving toward the furnace opening and negative moving toward the gas inlet) with respect to the wafer position (considered at zero position). The temperature profile was done with no gas flow into the chamber. At the position that the wafers were actually placed, the temperature was T°C±1.5%. The temperature profile was done using a type K thermocouple.

The last major parameter investigated was the placement of the wafers in the quartz tube. There were two factors considered: wafer placement parallel or perpendicular to the gas flow, and the number of wafers to be oxidized at one time. When a wafer was tested for a parallel orientation with the gas flow, the oxide layer was found to have a very observable color gradient from one side to the other. On the other hand, the oxide layer appeared to be very uniform when the wafer was oriented perpendicular to the gas flow. Additionally, wafers were oxidized individually and in groups both with and without dummy wafers. Even though wafers oxidized in groups were approximately only 3/16" apart from each other, they did not oxidize at the same rate based on color observations. However, wafers appeared very similar in color from run to run when the wafers were oxidized individually at the same position in the furnace.

It was concluded that the optimum parameters for this furnace for oxidizing of the thin film tungsten wafers were:

1. Oxygen gas flow at 0.475 liters/min
2. Placement of the wafers 22.5" from the furnace opening

3. Single wafers oxidized in the furnace
4. Wafers placed perpendicular to the gas flow

The last major consideration was the processing of the wafer. A detailed step-by-step procedure is described in Appendix C. Basically, undelineated pieces of tungsten film samples from both the U of A and SNL were cleaned and then oxidized. The oxidized wafers were then used for thickness measurements on the Randolph AutoEL^{R}-II Ellipsometer. The pieces that were delineated had a test pattern on them and were used to do physical thickness measurements before and after oxidation using a Tencor Alpha Step.

Tungsten Oxidation

The oxidation rate of tungsten tends to follow four regional descriptions: logarithmic, parabolic, linear, and evaporative as a function of time. The logarithmic region is described by

$$X_{ox} = K_1 \ln (t)$$

where K_1 is the logrithmic rate constant and t is the time of oxidation. In this region, the oxidation of tungsten is due to ambient oxygen and temperature. The mechanism for this oxidation is not well defined, but most probably this growth takes place due to chemisorption (Kofstad 1966). This logarithmic region occurs until a thickness of approximately 50Å (native oxide). The chemisorption process, which typically forms a few monolayers of oxide is considered to be caused by the

dissociation of oxygen molecules which are then ionized. The oxygen acquires electrons from the metal which forms an electric field causing ions to drift across the forming oxide film. As the film becomes increasingly thicker, the electric field has less effect on the growth mechanism (Scully 1966).

The next regions of growth are the parabolic region and the linear region of oxidation. These two regions can be described generally by the mathematical equations

$$X_{ox}^2 = K_2 t + D$$

and

$$X_{ox} = K_3 t + C$$

respectively, where K_2 is the parabolic rate constant, K_3 is the linear rate constant, t is time, and C and D are $X_{ox}(0)$, which is considered to be the native oxide. There are two mechanisms which are considered to be the driving force for oxide growth in these regions. The first is a concentration gradient and the other is stresses in the protective scale that causes cracking to occur in the oxide film. Generally, the concentration gradient is considered to be the most important factor in the region of parabolic oxide growth. This typically occurs at temperatures below 500°C. The linear growth occurs between 500°C and 1000°C (Gulbransen and Andrew 1960, Jepson and Aylmore 1961). The

mechanism for this oxide growth appears to be that the protective scale grows to a critical thickness and then cracks, allowing additional diffusion of oxygen to the metal surface. This process occurs over the oxide surface (Jepson and Alymore 1961).

Oxide growth in the parabolic and linear regions consist of different compositions, typically WO_2, $W_{18}O_{49}$, and WO_3 (Kofstad 1966). As the scale starts to grow, a protective scale forms first followed by a more porous oxide which is typically WO_3. Figure 3 shows a typical layer composition of tungsten oxide. The oxide that is closest to the gas interface is the most oxygen enriched species.

The last region of tungsten oxidation takes place at temperatures above 1000°C. In this region, evaporation takes place as oxidation occurs. The oxide evaporation can take place at the same rate of oxidation (Kofstad 1966).

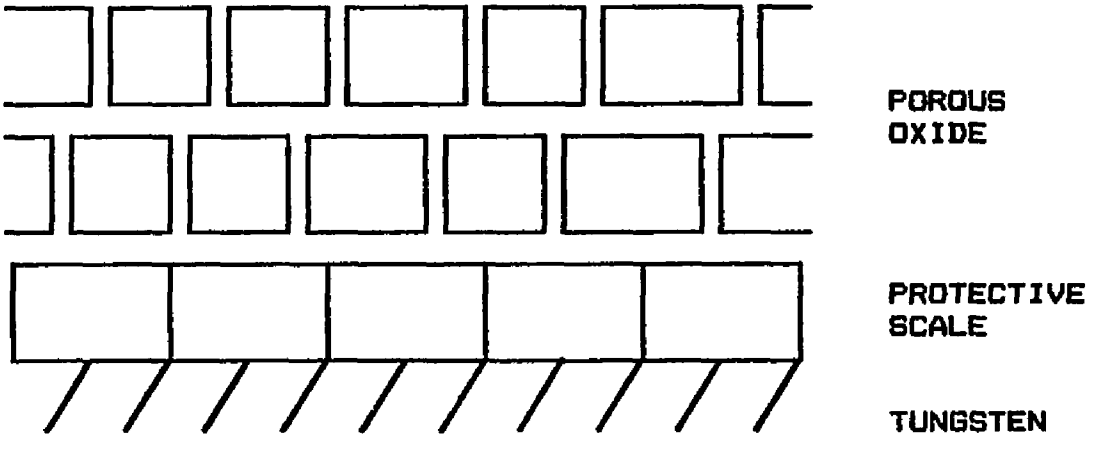

Figure 3. Typical Layer Composition of Tungsten Oxide.

The oxidation of tungsten described above in all regions is a function of temperature, pressure, time, crystal structure, and surface preparation. Of these variables, only temperature and time will be considered in this study.

Results

Upon completion of the oxidation run, the oxide thickness was measured using a combination of two methods. The Tencor Alpha Step was used prior to oxidation and after oxidation as a physical measurement. In addition, a Rudolph AutoEL^{R}-II ellipsometer was used to give the corresponding thickness optically. The data used for the oxide thickness measurement analysis was obtained from the optical measurements. The physical measurements were used to determine the corresponding order from the ellipsometer output. See Appendix B for a description and related equations for the ellipsometer measurements. The data presented in Table 2 is the optically measured oxide thicknesses for both the U of A and the SNL samples.

Additionally, Rutherford Backscattering (RBS) was done on several samples from both U of A and SNL. The RBS was done in the physics department at the University of Arizona. (A description of RBS can be found in Appendix A.) The thickness found by RBS is shown in Table 3.

The trends in the measurements are the same as the physical and optical thickness measurements. The difference in the measurements could be accounted for by considering the following:

1. The interface thickness was not accounted for in the RBS.

Table 2. Optically Measured Tungsten Oxide Thickness

TEMP (°C)	TIME (MIN)	THICKNESS (Å)	
		SNL	U of A
300	10	28	48
300	50	70	124
300	90	107	163
375	10	103	178
375	50	272	406
375	90	477	584
375	130	516	700
450	10	513	571
450	50	1000	2000
450	90	1629	2831
450	130	1808	3135
525	10	1375	3183
525	50	2789	4453
525	90	2987	5850

Table 3. RBS Thickness Measurements

TEMP (°C)	TIME (MIN)	THICKNESS (Å)	
		U of A	SNL
450	50	980	750
450	90	1380	1150

2. Assumed that the outside oxide was WO_3 and the corresponding density was assumed.
3. The error in using the Alpha Step and the ellipsometer combination for thickness measurements.

A comparison of this data to that for bulk tungsten can be done using data from the literature. The data given in the literature is in $\mu gm/cm^2$. To convert to Å, this data is multiplied by 67.5. The conversion factor is based on pure WO_3 being formed, a surface density of 7.16 g/cm^3, and a surface roughness ratio of approximately unity. The one major problem with this conversion factor is its validity for heavily oxidized samples. The reasons for this could be oxidation taking place more rapidly at the edges, the cracking of the oxide surface, and surface area reduction due to oxidation (Gulbransen and Andew 1960).

Table 4 and Table 5 are tables that show data converted from $\mu g/cm^2$ to Å taken from E.A. Gulbransen and K.F. Andrew and D.W. Jepson and D.W. Aylmore.

There are some important considerations when comparing literature oxidation rates to the rates found for thin tungsten films. The first major consideration is the literature data comes from oxidizing bulk tungsten. Additionally, the conditions of oxidation in the literature were done at reduced pressure with unspecified gas flow. However, pressure has only a minor influence on the oxidation of tungsten at the temperature range of interest (Gulbransen and Andrew 1960).

One other factor that can influence the oxidation is preparation of the tungsten surface. The bulk tungsten prepared by W.B. Jepson and

Table 4. Bulk Tungsten Oxide Growth
(Jepsen and Aylmore 1961)

TEMP (°C)	THICKNESS (Å)				
	25 min	50 min	75 min	100 min	125 min
500	5400	7425	8775	9787	10463
600	23625	33750	43875	54000	63450

Table 5. Bulk Tungsten Oxide Growth
(Gulbransen and Andrew 1960)

TEMP (°C)	THICKNESS (Å)			
	5 min	10 min	60 min	180 min
500	952	1458	4725	9585
550	2450	3645	11408	23828
600	4550	8033	31928	68850

D.W. Alymore was from Tungsten Manufacturing Company LTD, England. Samples were 20mm x 9mm which had been hot sheared from 0.8mm thick sheets. The main impurity was iron (0.05% max) with traces of other elements. These samples were also etched in aqueous solution of potassium ferricyanide and caustic soda then rinsed in water and acetone (Jepson and Alymore 1961). The samples that were prepared for E.A. Gulbransen and K.F. Andrew were prepared from Westinghouse high purity 5 mil cold rolled tungsten sheet or 9 mil wire. The samples were sheared primarily by hot shearing followed by a tungsten etch containing NaOH and $K_3Fe(CN)_6$. This was used to remove scale formed by heating during the shearing operation. These samples were rinsed in DI water. The surfaces of these samples were polished with emery paper through 4/0 and finally cleaned with petroleum ether and absolute alcohol. Refer to Appendix C for the cleaning and preparation method used in this investigation.

The oxidation data obtained both physically and optically for both the U of A and SNL samples are plotted in Figure 4 through Figure 7. These are linear plots of oxide thickness versus time for the samples. In these graphs, it is very difficult to tell if the oxidation follows a parabolic or a linear relationship. In order to determine the relationship, the data were replotted in a parabolic form--oxide thickness squared versus time. This is shown in Figures 8 through 11.

Again referring to the parabolic equation

$$X_{ox}^2 = K_2 t + D,$$

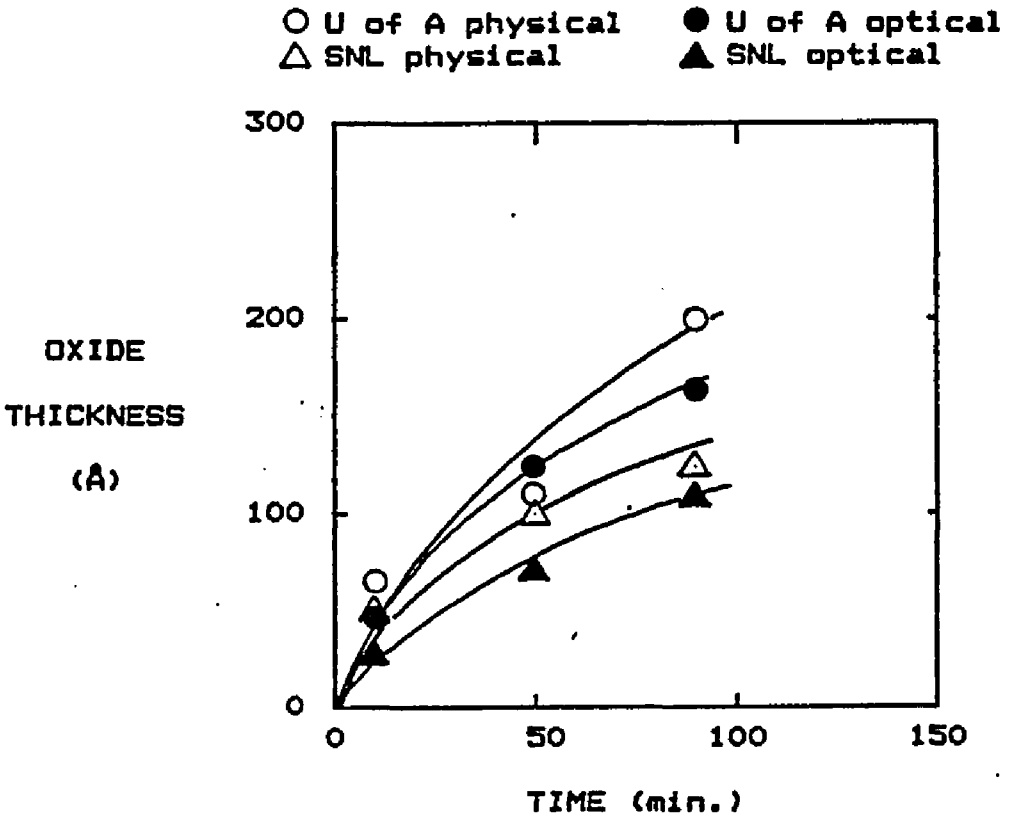

Figure 4. Linear Oxide Growth Curves for 300°C.

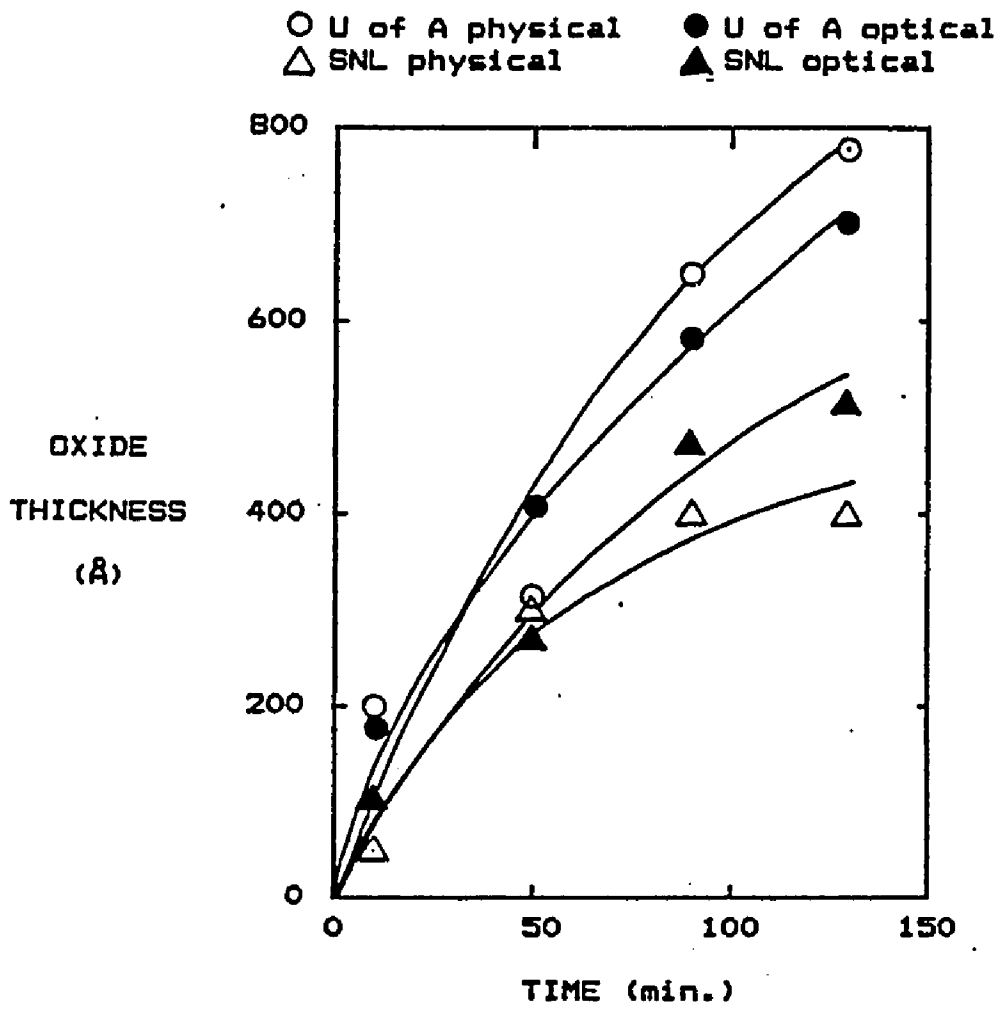

Figure 5. Linear Oxide Growth Curves for 375°C.

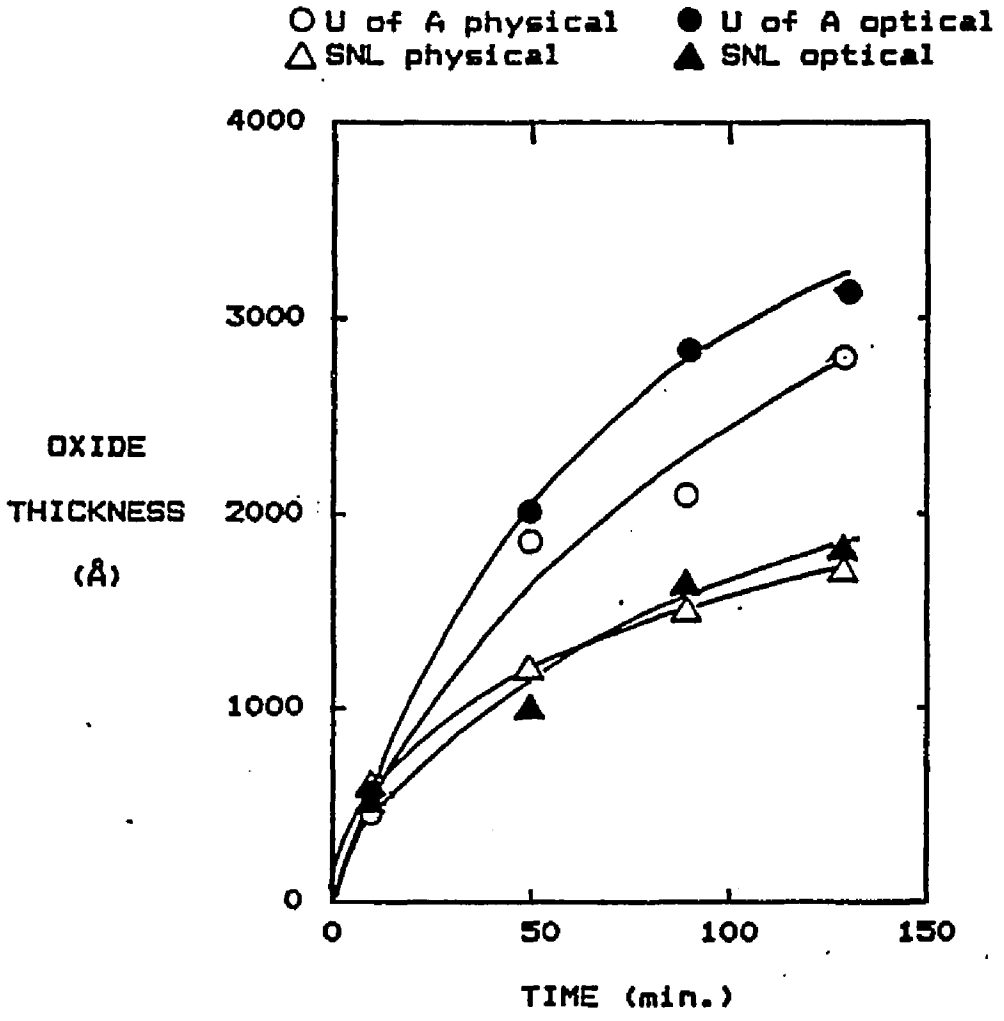

Figure 6. Linear Oxide Growth Curves for 450°C.

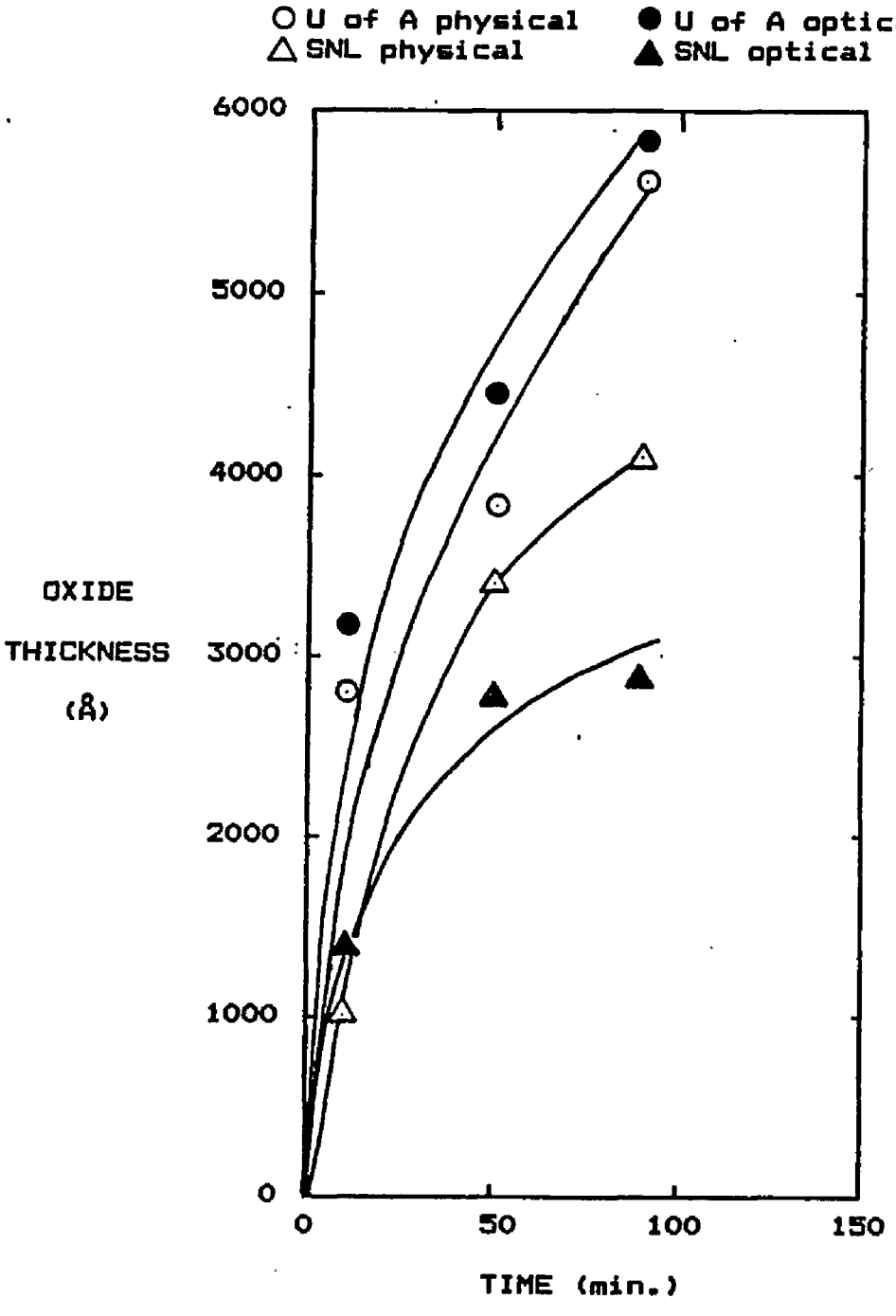

Figure 7. Linear Oxide Growth Curves for 525°C.

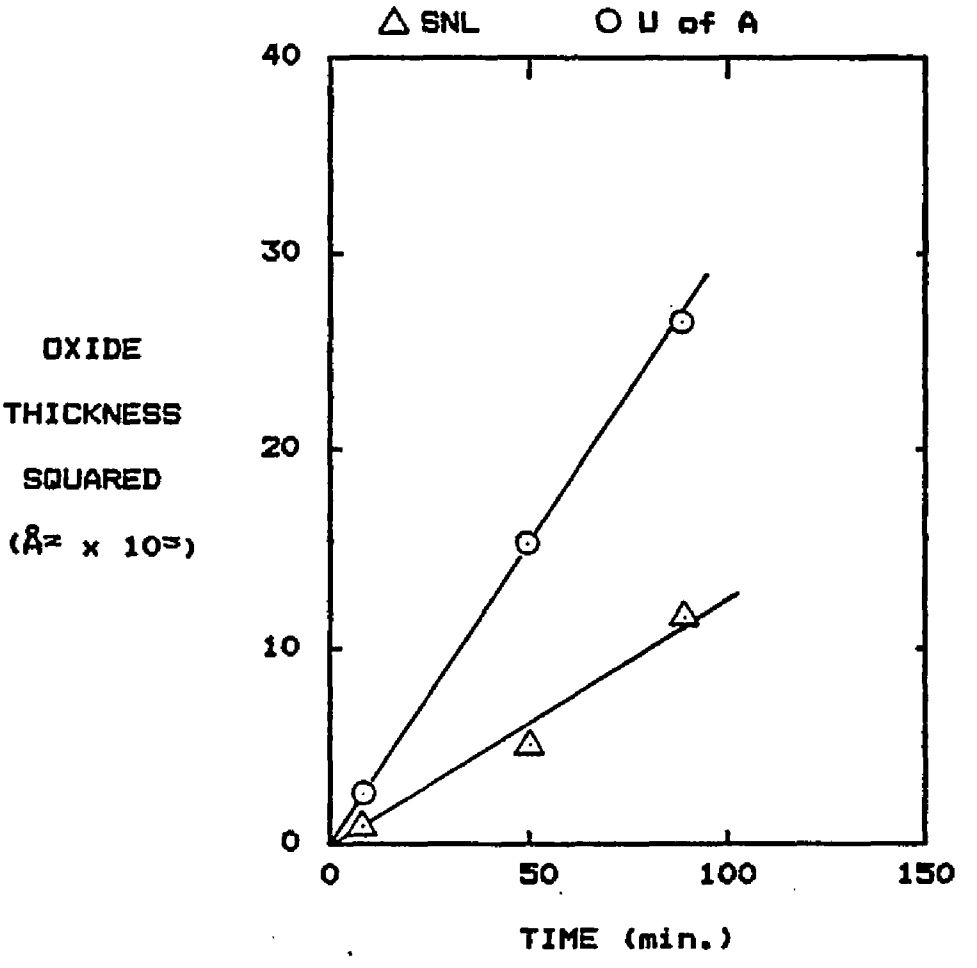

Figure 8. Parabolic Oxidation Curve 300°C.

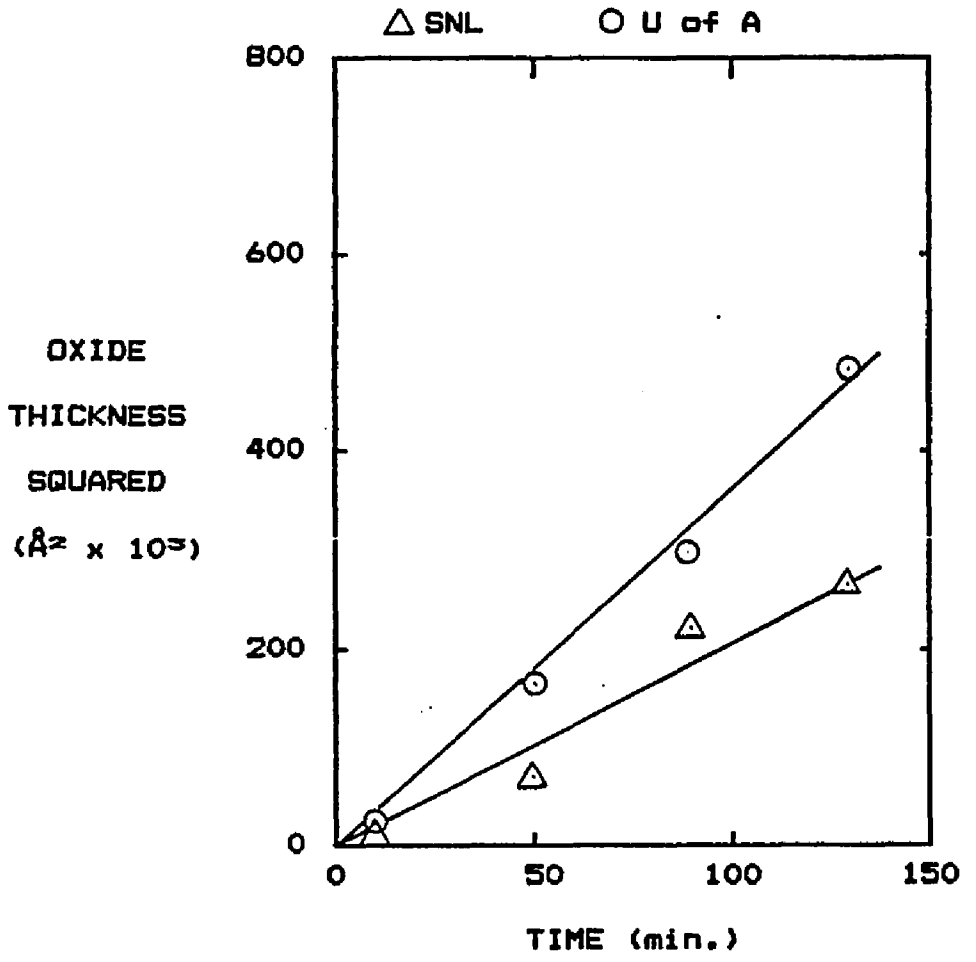

Figure 9. Parabolic Oxidation Curve 375°C.

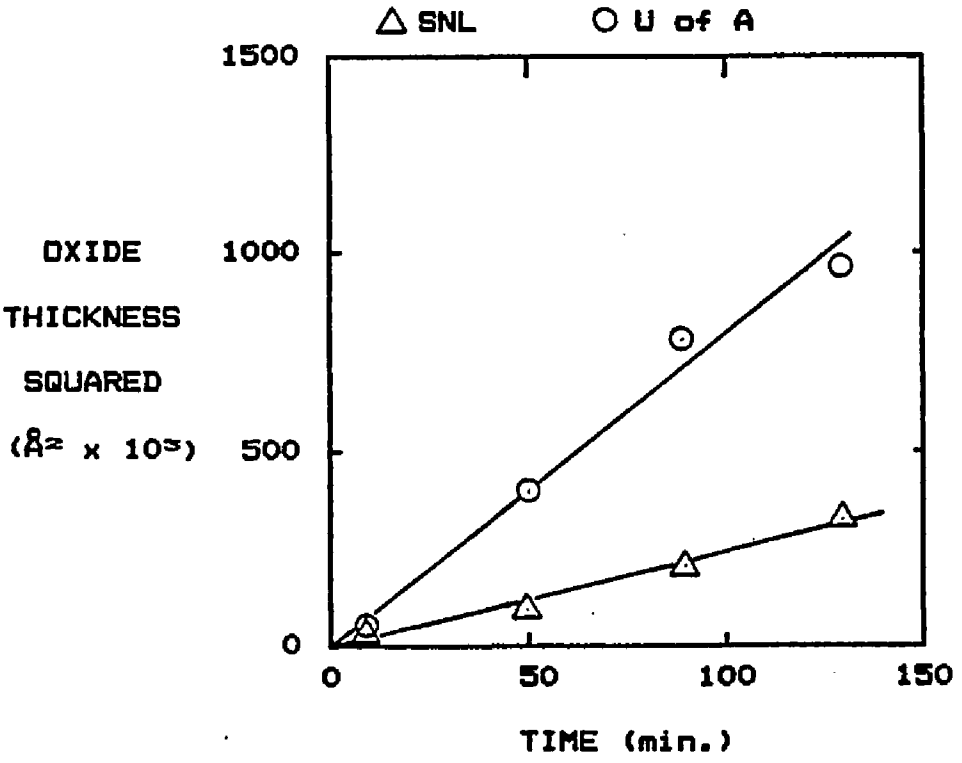

Figure 10. Parabolic Oxidation Curve 450°C.

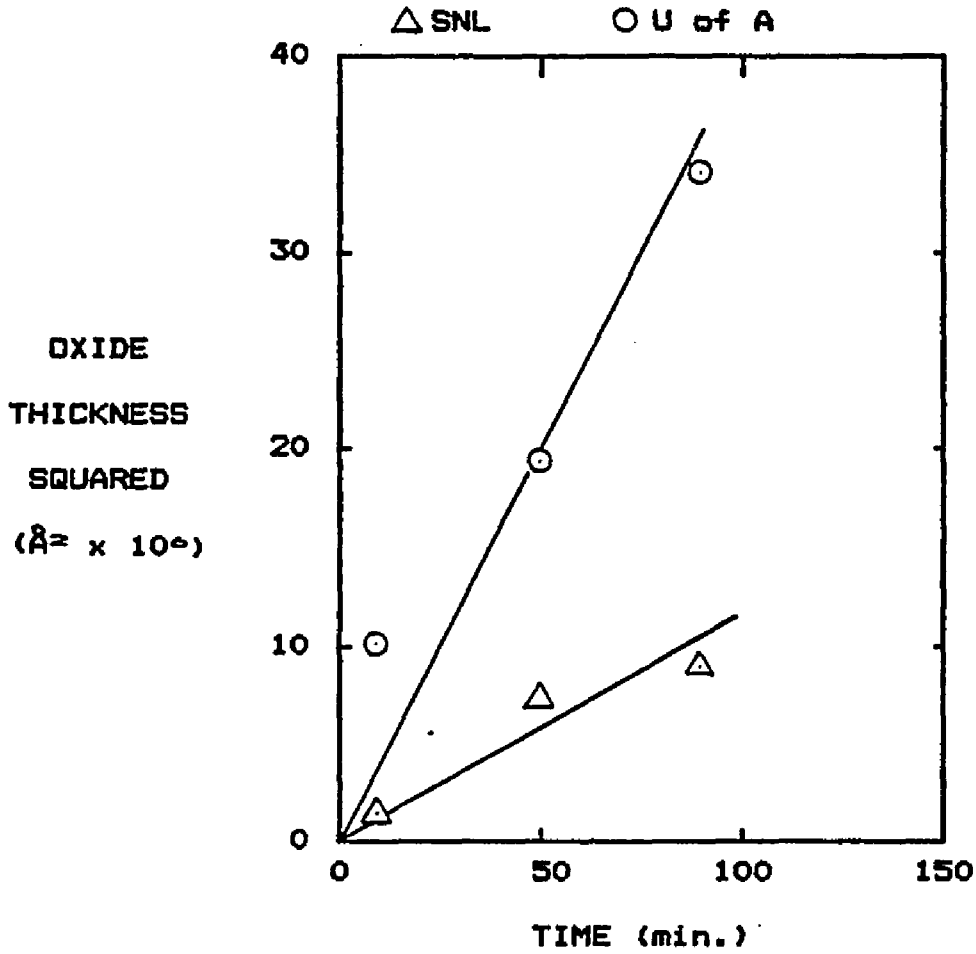

Figure 11. Parabolic Oxidation Curve 525°C.

D is assumed to equal zero. (This native oxide is very difficult to measure precisely given the techniques available for this investigation.) Therefore,

$$X_{ox}^2 = K_2\, t,$$

where the average parabolic rate constant is found by:

$$K_2 = \frac{\sum_{i=1}^{N} \frac{(X_{ox})_i^2}{t_i}}{N} \quad [\mathring{A}^2/\text{min}] \qquad \text{EQ. (1)}$$

Or the least squares fit value of the parabolic rate constant is calculated by:

$$K_2 = \frac{\sum_{i=1}^{N} (X_{ox})_i^2\, t_i}{\sum_{i=1}^{N} t_1^{\,2}} \quad [\mathring{A}^2/\text{min}] \qquad \text{EQ. (2)}$$

The data seem to fit this rate law as it looks linear on the plot of X_{ox}^2 versus time. Tables 6 and 7 are lists of parabolic rate constants for both the U of A and the SNL samples.

Table 6. Parabolic Rate Constant for U of A Samples

TEMP (°C)	PARABOLIC RATE CONSTANT ($Å^2$/min)	
	FROM EQ. (1)	FROM EQ. (2)
300	2.80×10^2	2.97×10^2
375	3.41×10^3	3.62×10^3
450	6.93×10^4	7.98×10^4
525	5.96×10^5	3.90×10^5

Table 7. Parabolic Rate Constant for SNL Samples

TEMP (°C)	PARABOLIC RATE CONSTANT ($Å^2$/min)	
	FROM EQ. (1)	FROM EQ. (2)
300	1.01×10^2	1.19×10^2
375	1.78×10^3	2.13×10^3
450	2.53×10^4	2.59×10^4
525	1.45×10^5	1.13×10^5

The parabolic rate appears to change by one decade for every 75°C change in temperature that occurs. The parabolic rate constant found by Gulbransen and Andrew for 500°C converted from $(\mu g/cm^2)^2$ sec^{-1} to $\mathring{A}^2/min$ is 3.53×10^5 $\mathring{A}^2/min$ and at 550°C it is 1.29×10^6 $\mathring{A}^2/min$. A trend that was also mentioned was that the parabolic rate constant changes with time. Basically, the only data in this investigation that supports this is the oxidation curve done at 525°C. When the parabolic rate is figured out on a point to point basis, the parabolic rate constant changes for the U of A samples from 1.01×10^6 $\mathring{A}^2/min$ for 10 minutes to 3.80×10^5 $\mathring{A}^2/min$ for 90 minutes. The SNL samples had a range of 1.89×10^5 $\mathring{A}^2/min$ to 9.91×10^4 $\mathring{A}^2/min$ for 10 and 90 minutes, respectively. One suggested mechanism for this phenomenon is that the oxidation of tungsten proceeds in two steps. The first is the growth of protective film followed by the growth of porous oxide. (See Figure 3.)

Activation energy is another figure of merit of the parabolic rate constant. To find the activation energy, a plot of the log (base ten) of the parabolic rate constant versus the reciprocal of temperature is made, as in Figure 12. The slope of the line shown in Figure 12 is Q/2.303R, where R = gas constant (1.986 Cal/K mole) and Q is the activation energy (Kofstad 1966).

From Figure 12, the activation energy for the U of A sample is 30,400 cal/mole and the SNL sample has an activation energy of 28,200 cal/mole. According to the literature, the heat of activation for the temperature range from 300°C to 500°C should be between 41,000 - 46,500

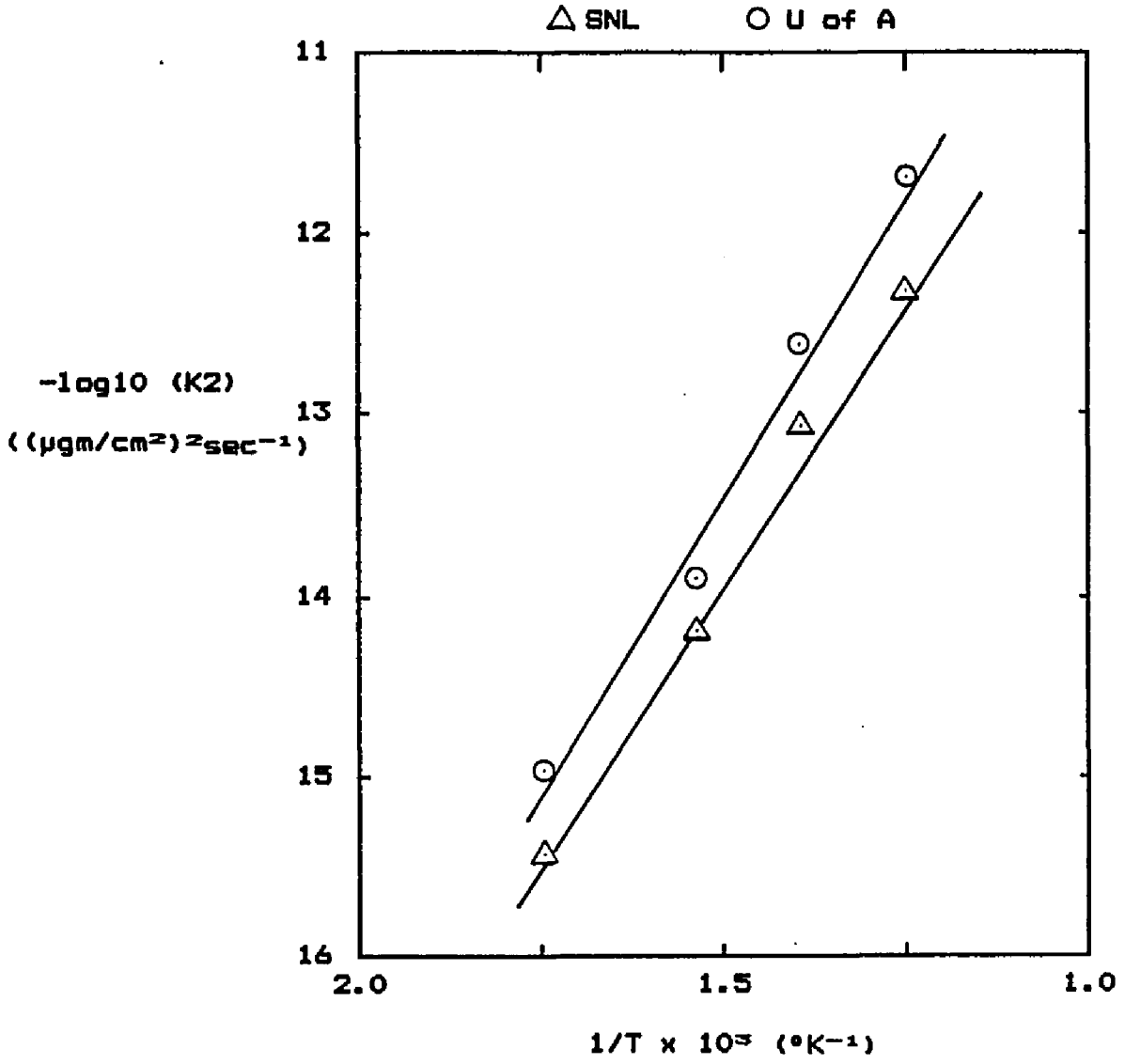

Figure 12. Log (Parabolic Rate Constant) Versus 1/T.

cal/mole (Gulbransen and Andrew 1960; Baur, Bridges, and Fassell 1956). The differences in the activation energies could be accounted for by (1) the data in the literature used more precise measurement techniques, (2) the conversion factor of 1/67.5 was used to convert Å to $\mu g/cm^2$ in order to plot the parabolic rate constant for the U of A and SNL samples, and (3) the bulk tungsten was less pure than the CVD tungsten films.

CHAPTER 3

CHARACTERIZATION OF TUNGSTEN OXIDE FILM

There are several properties of a thin film such as tungsten oxide one would like to characterize. These properties include the oxidation rate which was discussed in Chapter 2, the composition, the refractive index, and the electrical characteristics. Each of these properties will be discussed as it pertains to the U of A and SNL samples. These properties all appear to be a function of thickness with the exception of stoichiometry.

Composition

As reported by Gulbransen and Andrew and others, the oxidation of tungsten ultimately forms an outer porous film which is understood to be WO_3. This was also found to be the case for the U of A and SNL films. The stoichiometry and uniformity were investigated by using Rutherford Backscattering at the University of Arizona. (Details of the system and pertinent equations can be found in Appendix A.) Using this method, several things were determined about the film stoichiometry, uniformity, and interface. Due to limited resources, the RBS was only done on samples oxidized at 450°C for 50 and 90 minutes for both the SNL and U of A films. Ideally, of course, all samples should have been analyzed by RBS to check for film properties. At this point, it can only be assumed that the properties would be similar. Figure

13 is a typical RBS spectrum that will be referred to in the following discussion for different properties and parts of the spectrum.

The first property to be discussed is the stoichiometry. The stoichiometry of the tungsten oxide was determined by using the RBS results and a method of comparing heights between spectra for pure tungsten and tungsten oxide. The composition of the outer layer was found to be WO_3. Table 8 shows the different compositions found from the different samples. Additionally, the compositions were checked at different energies and θ. The composition appears to be WO_3, independent of the sample type and thickness. This compares favorably to bulk tungsten which oxidizes to an outer layer of WO_3.

The literature states that ultimately the color of WO_3 on bulk tungsten is yellow (Galbransen and F. Andrew 1960, Kellet and Rodgers 1963). Each sample oxidized from both U of A and SNL was observed for oxidation color uniformity. Also, a comparison was made between the undelineated piece to the delineated piece for run to run uniformity. In these cases, the colors were very similar in shade. This indicates that the same oxidation conditions were present and the wafers oxidized similarly, independent of preprocessing done on the samples. But, the ultimate colors of the oxide were dependent on the thickness of the oxide grown. Table 9 is a color chart with the approximate thickness and corresponding color. It should be noted that the color listed is a subjective interpretation of the film color. The color charts for bulk tungsten oxide are predominantly black with blue and green edges until long oxidation periods in which yellow seems to appear.

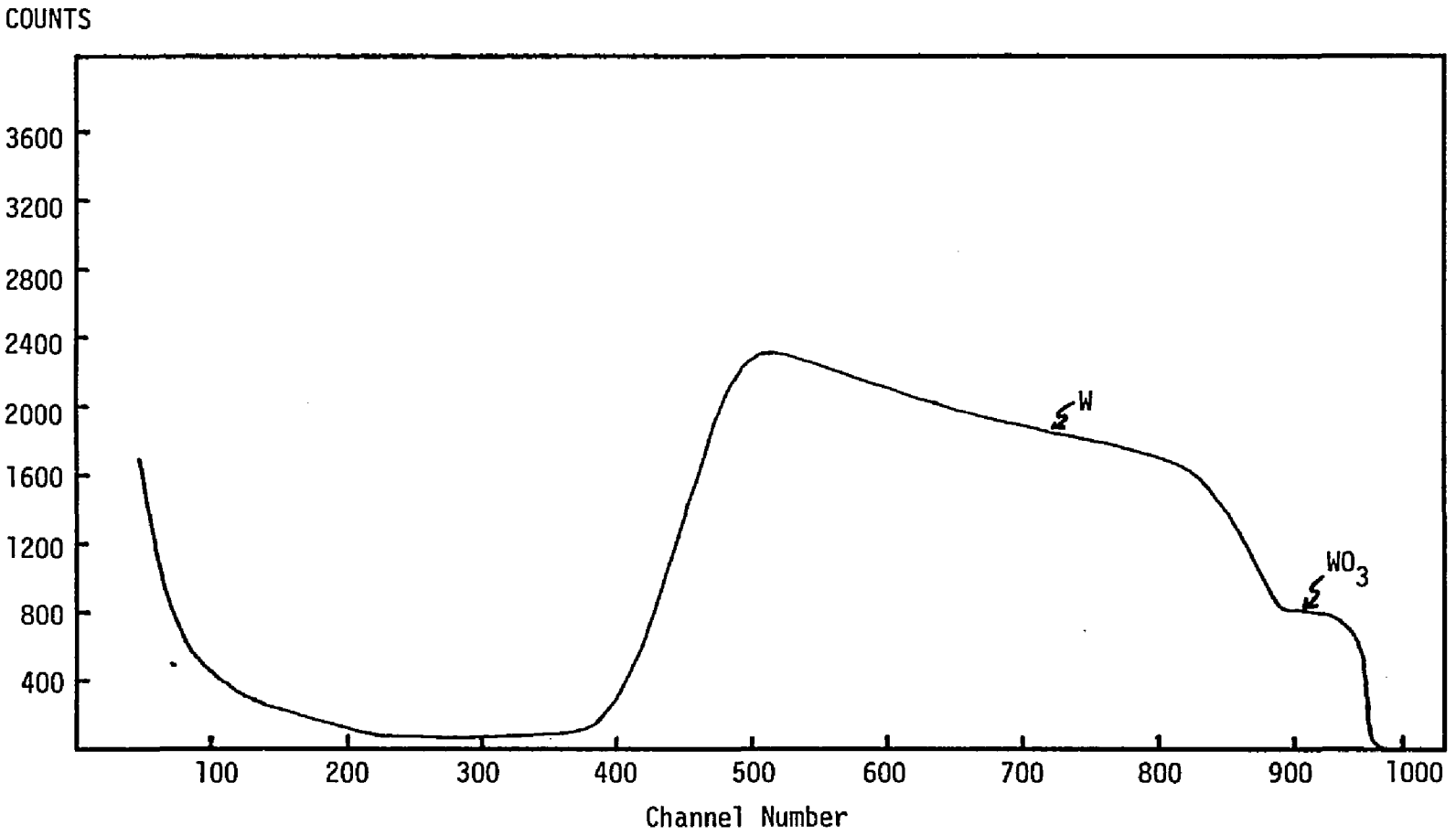

Figure 13. Rutherford Backscattering Spectrum.

Table 8. Stoichiometry of the Tungsten Oxide from RBS

TIME (MIN)	U of A	SNL	ENERGY, θ
50	$W_{1.00}O_{3.15\pm0.17}$	$W_{1.00}O_{3.10\pm0.17}$	1.892MeV θ=0°
50	$W_{1.00}O_{3.22\pm0.17}$		3.776MeV θ=45°
50		$W_{1.00}O_{3.13\pm0.17}$	3.776MeV θ=0°
90	$W_{1.00}O_{3.04\pm0.17}$	$W_{1.00}O_{3.15\pm0.17}$	1.892MeV θ=0°
90	$W_{1.00}O_{3.04\pm0.17}$		1.892MeV θ=45°
90		$W_{1.00}O_{3.04\pm0.17}$	3.776MeV θ=45°

Table 9. Color Chart of Tungsten Oxide

THICKNESS (Å)	COLOR
30	Pale Yellow
100	Gold
300	Orange Gold
500	Blue
600	Brown Gold
1000	Lemon Yellow
1400	Orange Purple
1700	Red Orange
2800	Purple
3000	Green
4500	Brown

One fact that was mentioned in the literature was that the edges seem to oxidize at a faster rate than the center. This was also found in both the U of A and the SNL samples. The color at the edges of individual pieces that were oxidized for longer times was typically a shade darker than the center zone. This could be due to cracking in the film or stress which would enable diffusion to occur at slightly faster rates.

Another point that can be brought out from the RBS spectrum is the interface between the WO_3 and the tungsten. In Figure 13, the zones are labeled to indicate where the tungsten, interface, and the WO_3 are present on the sample. The spectrum shows that the outer layer (WO_3) seems to be fairly uniform down to the interface between the WO_3 and pure tungsten. The interface does not have a uniform composition, and the composition changes from pure tungsten to WO_3. In addition, the interface appears to be fairly wide in comparison to the thickness of the oxide film present. Bulk tungsten oxide appears to have the similar structure of interface and uniform oxide covering.

Index of Refraction

The index of refraction was measured using a Rudolph AutoEL^R-II Automatic Ellipsometer at Sandia National Laboratories. The ellipsometer operates at a wave length of 632.8 nm with angle of incidence at 70°.

The refractive index was measured by first finding the index of refraction on the tungsten using the AutoEL^R-II. The assumption was made that the tungsten was an infinite film such that a single layer model was assumed. The general form of the index of refraction is $N_s \pm iK_s$

where N_s is the real part and K_s is the imaginary part. The imaginary part indicates the attenuation of the wave in the sample. The components of the tungsten film refractive index are:

	K_s	N_s
U of A	1.5	1.65
SNL	2.1	1.95

The real part of tungsten oxide refractive index is listed in Table 10. The index of refraction listed was the average value recorded for the sample, where three to four readings were taken, using an iterative process until the refractive index seemed to converge.

Figures 14 and 15 show the index of refraction graphically as a function of time. By looking at these figures, the only trend that seems to appear is that the index of refraction is greater as the tungsten oxide gets thicker. There are a couple of reasons that could account for the variability of the index of refraction: (1) the films appear to have a rough surface, (2) non-uniform WO_3 film across the surface of the wafer, and (3) the films are probably absorbing versus transparent which are the ideal films for which to use the ellipsometer for measurements. The ellipsometer used for the measurements is calibrated to measure the refractive index of single layer films on silicon. Examples of these films are silicon dioxide on silicon, silicon nitride on silicon, and photoresist on silicon. The tungsten oxide films in either the U of A or SNL case were not of this type. The U of A sample is WO_3-W-SiO_2-Si and the SNL sample is WO_3-W-Si which could cause different interactions at the interfaces.

Table 10. Tungsten Oxide Index of Refraction

TEMP	TIME	REFRACTIVE INDEX	
		SNL	U of A
300°C	10	1.728	1.314
300°C	50	1.809	1.602
300°C	90	1.966	1.578
375°C	10	2.302	1.432
375°C	50	1.875	1.479
375°C	90	1.820	1.47
375°C	130	2.206	4.236
450°C	10	1.995	1.876
450°C	50	-----	-----
450°C	90	4.146	1.688
450°C	130	3.127	5.255
525°C	10	2.769	4.179
525°C	50	6.106	2.414
525°C	90	9.626	2.434

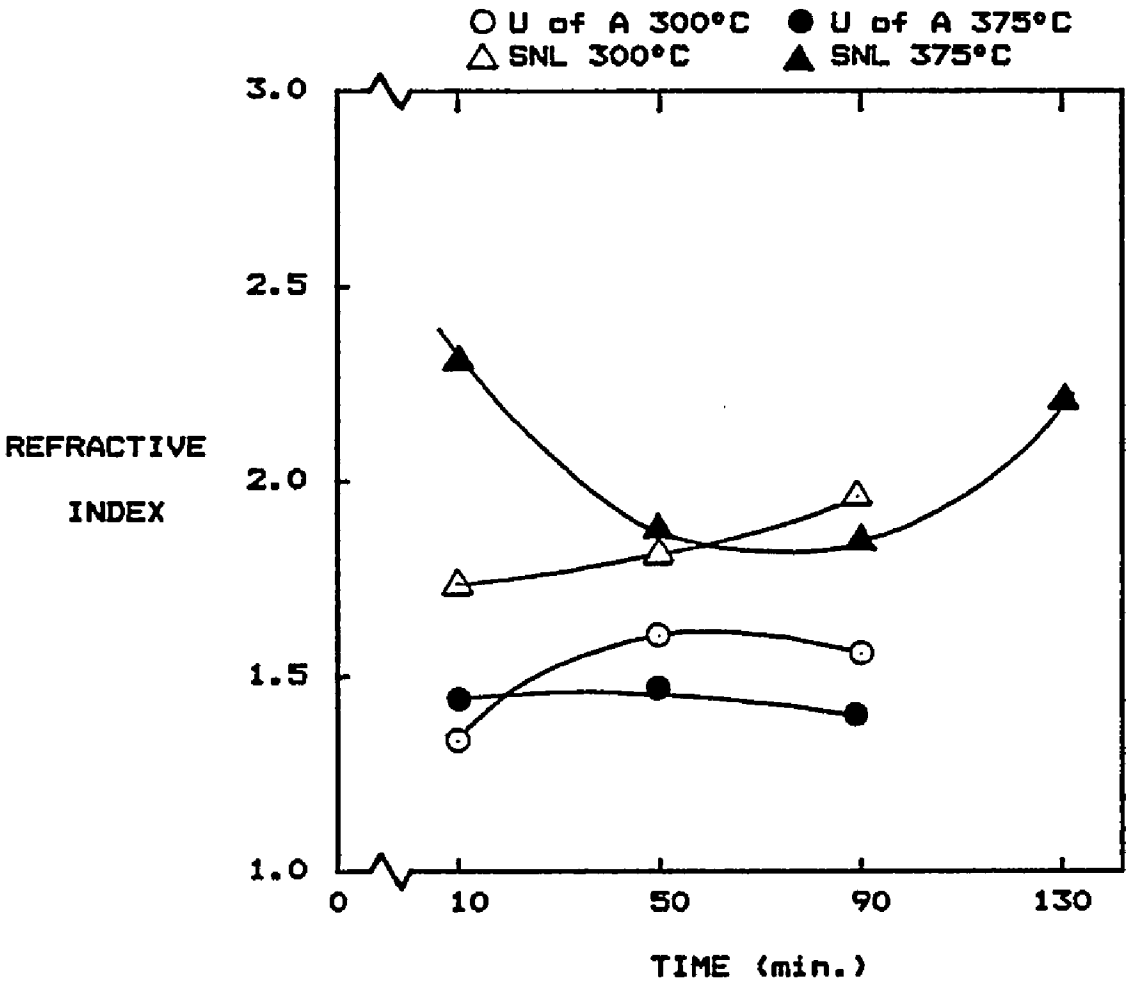

Figure 14. Refractive Index of Tungsten Oxide for 300° and 375°C.

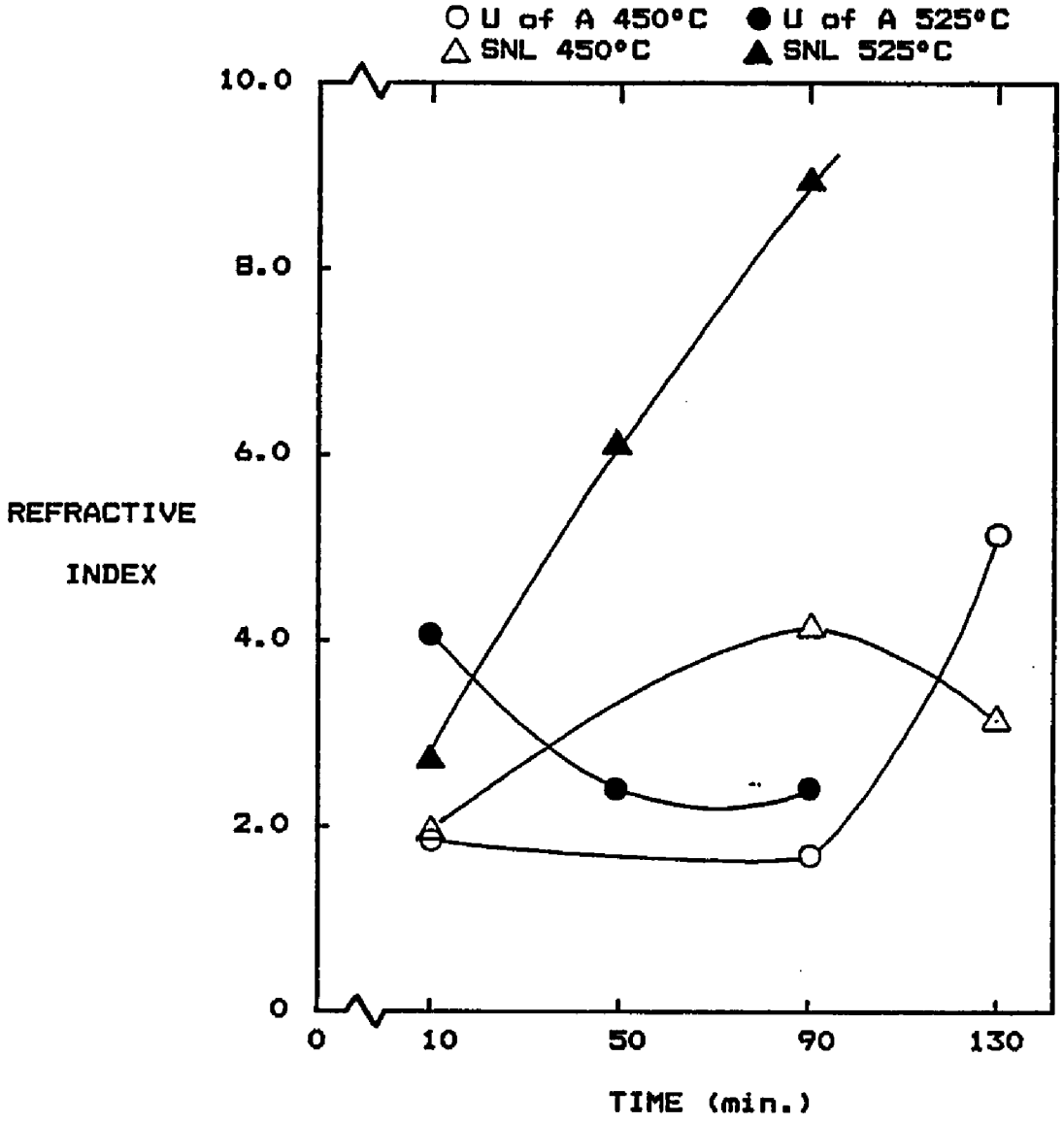

Figure 15. Refractive Index of Tungsten Oxide for 450° and 525°C.

Electrical Measurements

A major concern with using tungsten as a metalization layer for integrated circuit fabrication is that it oxidizes at about 300°C. In the case of using tungsten for part of a metalization scheme, the oxidation could affect the characteristics of the overall circuit. The electrical properties of tungsten oxide were measured by making a two wire measurement on a MOS capacitor used as a large area resistor. This is shown in Figure 16.

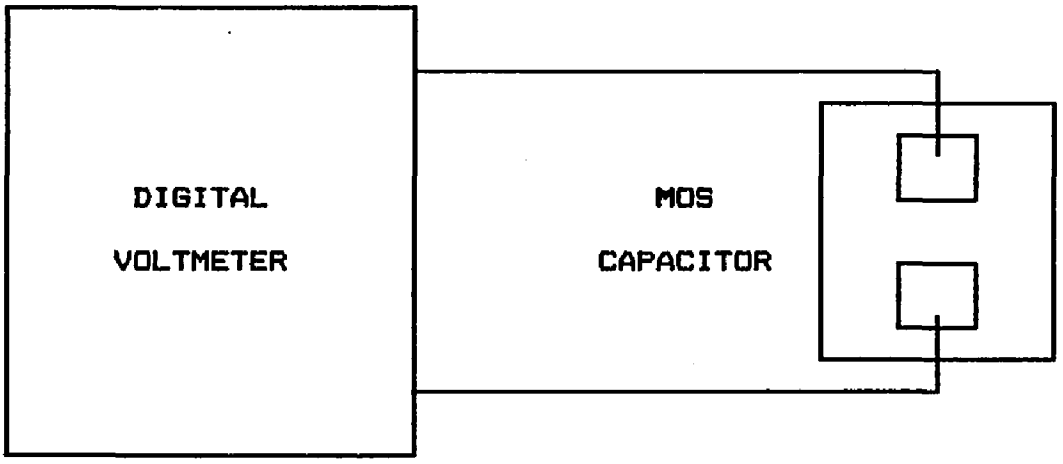

Figure 16. MOS Capacitor Used as Large Area Resistor for Resistivity Measurements of Tungsten Oxide.

During the course of the electrical measurements, problems occurred getting repeatable results from die to die on the same wafer. The results that were obtained should be used strictly as an estimate and not absolute values of resistivity. One of the factors that was ultimately considered part of the problem is the pressure with which the probes were applied to the device.

Prior to making the resistivity measurements, the wafers with tungsten oxide on them were coated with approximately 2000Å of aluminum and a standard photolithography procedure was used to delineate the electrodes of the MOS capacitor. The electrode areas were 250μm x 450μm. During the course of the investigation, there was found to be no convenient way to selectively etch the WO_3 without etching the tungsten. Therefore, the electrical measurements were made from aluminum pad to aluminum pad using the vertical structure of Al-WO_3-W-WO_3-Al as the resistor.

Figure 17 shows the vertical structure of the measured resistors, where R is the resistance of the SiO_2 on the U of A wafers and silicon on the SNL wafers. In either case, it was assumed that the resistance due to the tungsten and the aluminum was a short circuit.

Using a two probe measurement, a resistance was measured first with both probes on one pad. This was considered to be the system resistance. The average system resistance for the SNL sample is 2.86Ω. The average system resistance for the U of A sample is 1.66Ω. These pad to pad measurements were made at four places on each die, and the variation was relatively small. In each case, ten measurements were taken at random places on the sample. For each measurement, the system resistance was subtracted from the measured value; and the resulting resistance was divided by two to get R_{WO3}. The resistivity was then calculated by equation 3.

$$\rho = \frac{AR}{d} \qquad \text{EQ. (3)}$$

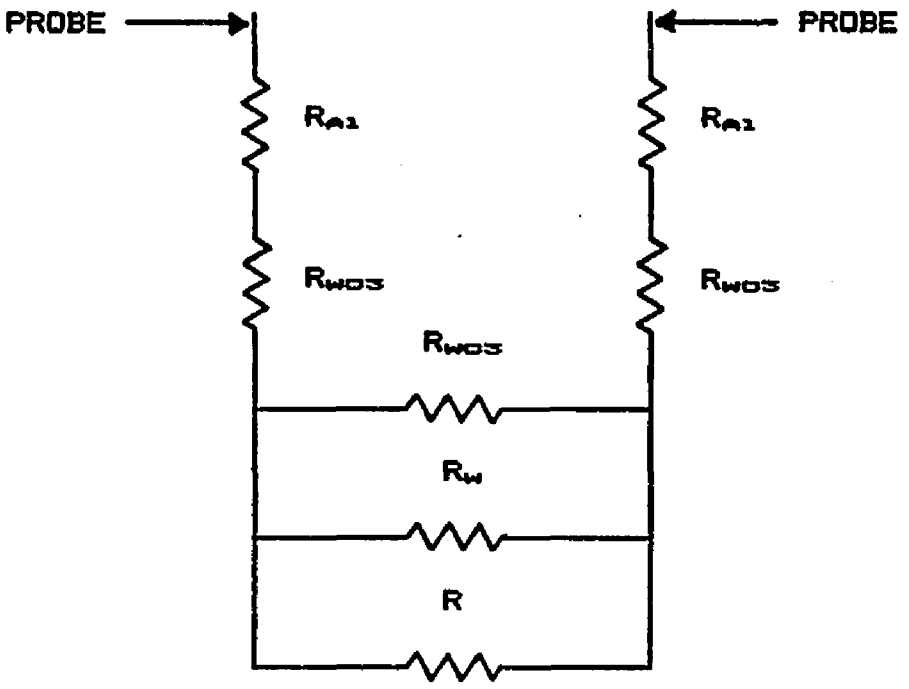

Figure 17. Electrical Structure for Measurement of Tungsten Oxide Resistivity.

Where,

ρ = resistivity in Ω-cm,

R = resistance,

A = pad area, and

d = oxide thickness.

Tables 11 and 12 show the average resistivity of the samples using the above technique.

In all cases, the SNL samples had a higher resistivity than the U of A samples. Additionally, the U of A samples seemed to be more consistent in changes of magnitude. There are several properties inherent to the material that could cause these large changes in the resistivity. The first would be the crystal structure of the WO_3. The second property would be the WO_3-W interface and whether or not this is sharp. If the interface was not sharp, probe placement could cause variation in the resistance measurements. And the third property could be that there is some interaction (primarily noise) from silicon in the SNL samples whereas the U of A samples were isolated by a SiO_2 layer. It should be noted that there is some thought that the WO_3 formed in the oxidation process is an n-type semiconductor (Kubaschewski and Hopkins 1960).

The crystal structure and interface were investigated briefly by SEM (using Robinson Backscattering) photographs taken by SNL on two samples. In both cases the interface appears to be very rough, and the crystal structure of the U of A samples was larger than SNL. Additionally, the surface of the sample appeared to be rough and

Table 11. WO_3 Resistivity for SNL Samples

TEMP	TIME	MEAN RESISTIVITY (Ω-cm)	STANDARD DEVIATION (Ω-cm)
300°C	10	5580	3270
300°C	50	14600	8080
300°C	90	11400	4970
375°C	10	4120	3220
375°C	50	895	893
375°C	90	746	765
450°C	10	297	150
450°C	50	346	310
450°C	90	---	---
525°C	10	133	129
525°C	50	56	26
525°C	90	127	95

Table 12. WO_3 Resistivity for U of A Samples

TEMP	TIME	MEAN RESISTIVITY (Ω-cm)	STANDARD DEVIATION (Ω-cm)
300°C	10	1150	431
300°C	50	240	133
300°C	90	238	56
375°C	10	---	--
375°C	50	46	15
375°C	90	45	14
450°C	10	107	36
450°C	50	21	3
450°C	90	11	1
525°C	10	12	1
525°C	50	13	2
525°C	90	6	4

non-uniform. In some areas of the sample, it appears as if the top layer of oxide was cracking. This could definitely account for the problems that were encountered because of changes in pressure on the probes and the varied resistance measurements.

CHAPTER 4

PASSIVATION OF TUNGSTEN FILM

One of the current problems with the use of tungsten is the degree of passivation required during integrated circuit fabrication after tungsten deposition. There are numerous materials and techniques that can be used to prevent the oxidation of tungsten. During the course of this investigation, CVD silicon dioxide and LPCVD silicon nitride were used as passivating films. In choosing either of these films as a means of passivation, the following considerations should be taken into account (Hass and Thun 1969).

1. It should match the coefficient of thermal expansion.
2. It should be insoluble in attacking medium.
3. It should be impervious to attacking medium.
4. The method of deposition should be compatible with IC processing.

These four criteria are met by the use of either silicon nitride or silicon dioxide. This process was only done on U of A samples.

The CVD silicon dioxide was deposited using a Rotox 60. This system had a three cycle process: preheat, deposit, and cool down. The process was done at 420°C. The oxide was deposited using a chemical reaction of

$$SiH_4 + O_2 \longrightarrow SiO_2 + H_2$$

This oxide that was deposited was a more porous oxide than a thermally grown oxide. Additionally, the oxide appeared to have an uneven thickness across the surface of the wafer. Three oxide thicknesses were used on delineated wafers: 2200Å, 4000Å, and 6200Å. The wafers were then placed in a furnace for one-half, one, and two hours at 400° and 500°C. Prior to the oxidation run, a sample at each deposition time was etched in buffered HF to check that deposition process does not cause the tungsten to oxidize. In all three cases, the change in resistance was less than 1% with either the ten square or 524 square four probe resistor. But there was slight color change in the tungsten.

Silicon nitride was deposited using cold wall LPCVD. The chemical reaction done at about 800°C is:

$$3SiH_4 + 4NH_3 \longrightarrow Si_3N_4 + 12H_2$$

The deposition rate was approximately 100Å/min. Two thicknesses of Si_3N_4 were used: 400Å and 2000Å. The samples were put in a furnace for oxidation at temperatures of 500°, 700°, and 800°C. Again, a sample of both thicknesses was etched in hot phosphoric acid. The resistance change actually was a slight decrease of about 1%. This could be an annealing effect due to the deposition process. There was no color change after the nitride etch for tungsten.

In both cases of passivation, the tungsten films that were used were 1500 to 3000Å thick. Additionally, two sizes of Kelvin resistors were measured: a ten square resistor of approximately 4.5

to 10 Ω and a larger resistor of 524 squares of approximately 200 to 300 Ω. The resistance of these resistors depended on the thickness of the tungsten. The technique used to measure the resistance is shown in Figure 18.

A current of approximately 1ma was forced through the resistor. Additionally, four die were measured prior to deposition and the same four die were measured after oxidation and etch of the passivating film. An average of each measurement was compared for change in resistance versus oxidation time. Positive change indicates an increase in resistance after oxidation; on the other hand, negative change indicates a decrease in resistance with respect to the original resistance. Figures 19 through 22 are plots of the percent of change in resistance with respect to the temperature at which the devices were tested for silicon dioxide and silicon nitride passivation layers. One point that needs to be noted is that in some cases the silicon nitride at the thickness of 450Å partially lifted at the 700°C oxidation temperature. There were still several die in each case that could be measured and this was done. Additionally, all oxidation was done in a saturated furnace with two liters/min of oxygen at the respective temperature.

In all passivation tests, the silicon nitride was a better means of passivation than silicon dioxide. There was no oxidation with 2000Å of silicon nitride subjected to a temperature of 800°C. This is not surprising since silicon nitride tends to be a better diffusion mask against oxygen than SiO_2. Additionally, silicon nitride tends to have a lower defect density than CVD silicon dioxide. This helps

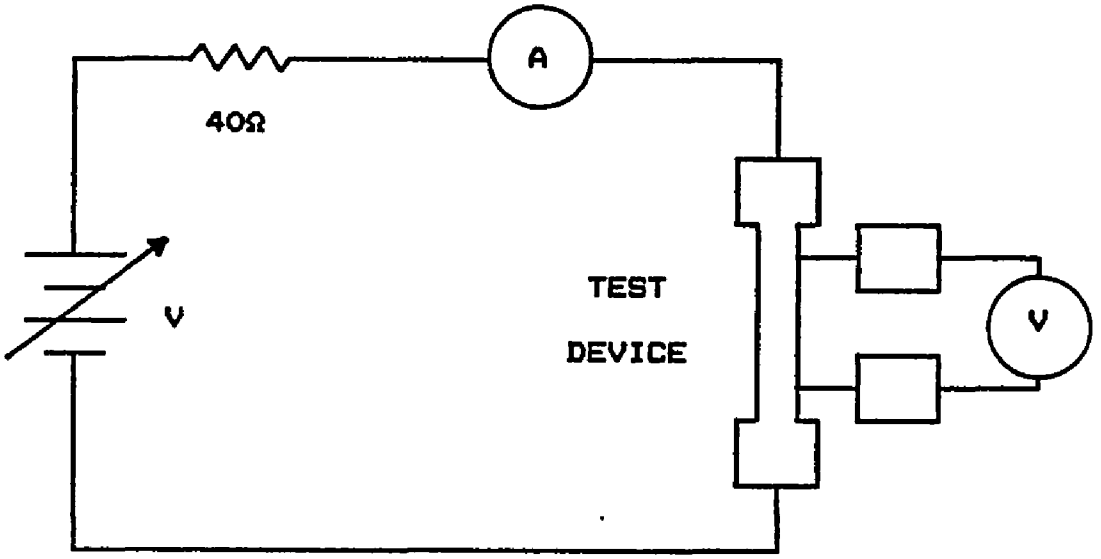

Figure 18. Electrical Test with Kelvin Resistor.

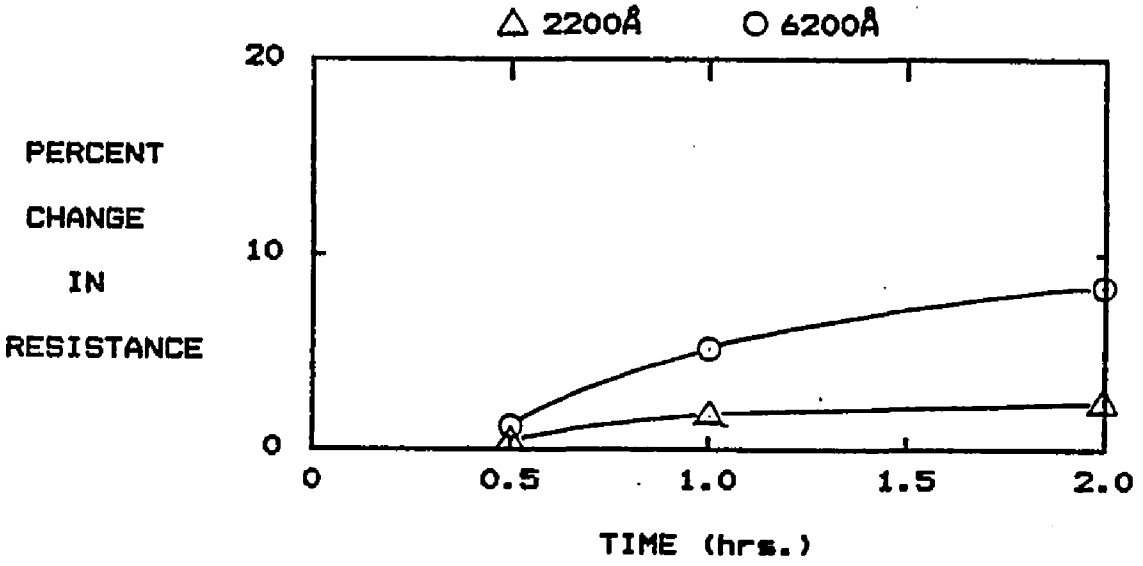

Figure 19. Percent Change in Resistance of Tungsten Resistor Passivated with Silicon Dioxide and Oxidized at 400°C.

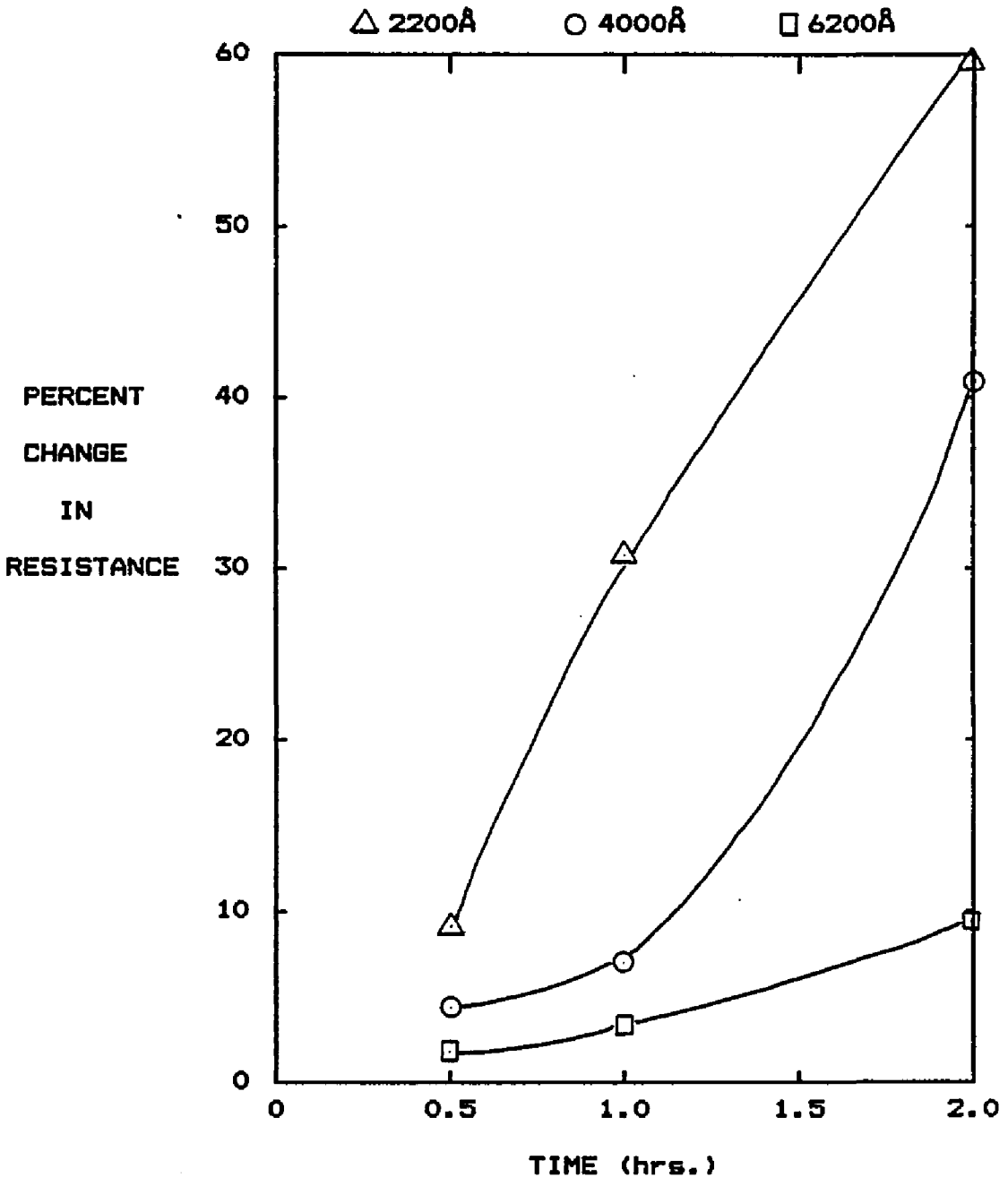

Figure 20. Percent Change in Resistance of Tungsten Resistor Passivated with Silicon Dioxide and Oxidized at 500°C.

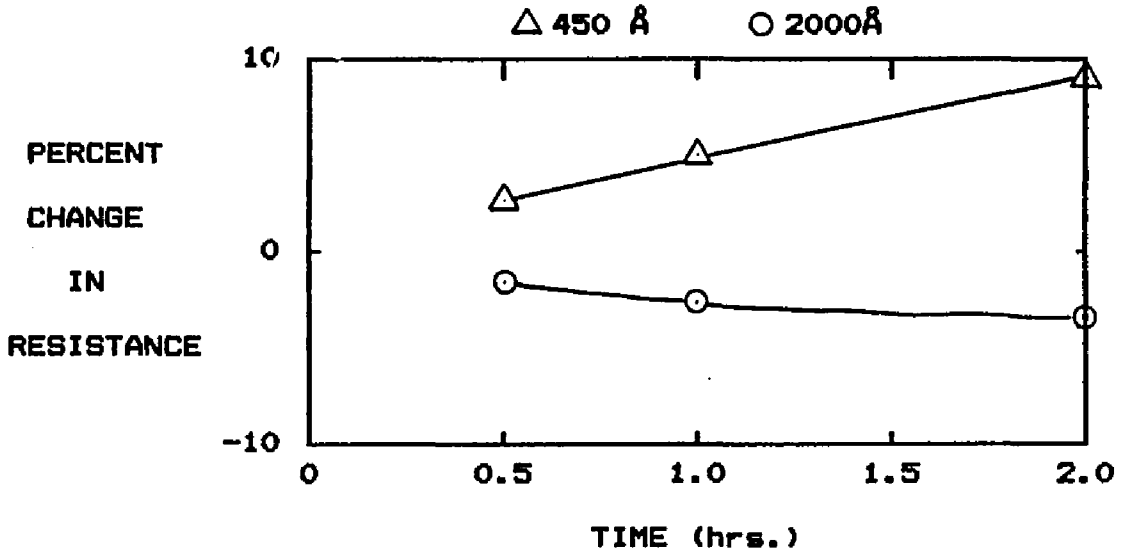

Figure 21. Percent Change in Resistance of Tungsten Resistor Passivated with Silicon Nitride and Oxidized at 500°C.

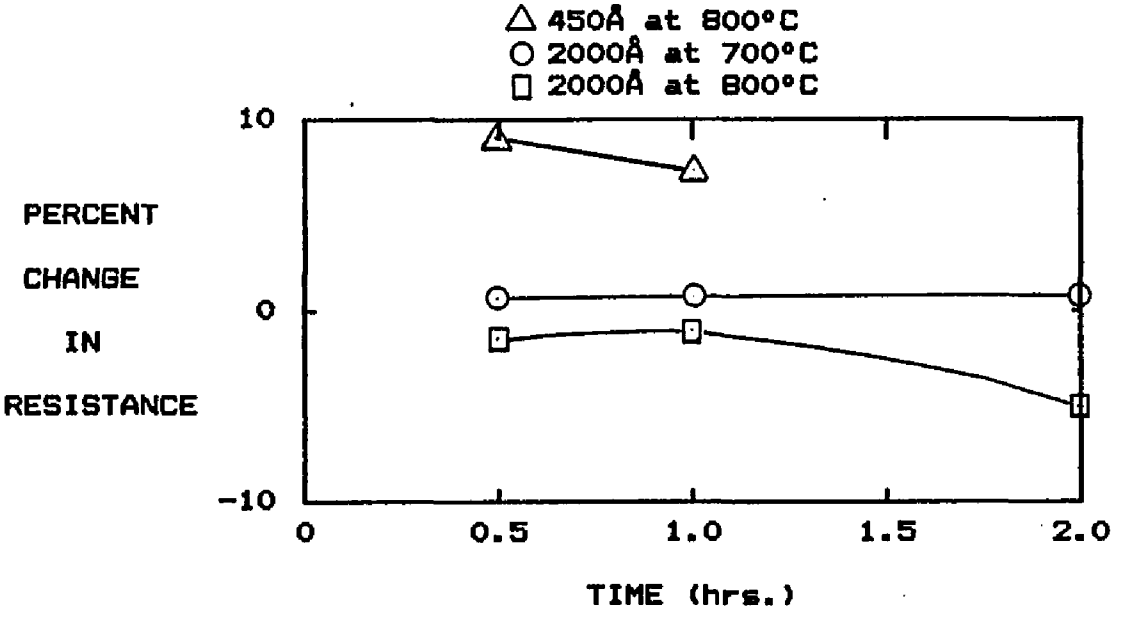

Figure 22. Percent Change in Resistance of Tungsten Resistor Passivated with Silicon Nitride and Oxidized at 700° and 800°C.

reduce possible defect sites where impurities can diffuse into the metal surface (Milek 1971). This is similar to results that were found for silicon, that silicon nitride is a better material to be used for passivation than silicon dioxide for silicon surfaces (Deal, Fleming, and Castro 1963). One other trend that seems to occur with the thicker silicon nitride is that the resistance seems to decrease slightly for the devices oxidized at elevated temperatures. This could be due to annealing effects at the higher oxidation temperature.

CHAPTER 5

SUMMARY

The objective of this thesis was to characterize the oxidation of thin film tungsten. The investigation used two types of samples. The first type of sample was a cold wall LPCVD tungsten deposited on SiO_2 processed at the University of Arizona. The second type of sample was processed at Sandia National Laboratories and used hot wall RPCVD tungsten deposited on silicon. The oxidation of the two film types was done for 10, 50, and 90 minutes at temperatures between 300° and 525°C in 75°C increments in one atmosphere of oxygen.

The oxide was grown and measured for the different points in the matrix. The oxide growth rate was found to be parabolic at all temperatures of interest which compared favorably to the literature for the oxidation of bulk tungsten. In all cases, the U of A samples grew thicker oxide for a specific time and temperature than did the SNL samples. The parabolic rate constant ranged from 2.86×10^2 $\mathring{A}^2$/min to 5.96×10^5 $\mathring{A}^2$/min for the U of A samples whereas the SNL samples had a parabolic rate constant that ranged from 1.01×10^2 to 1.45×10^5 $\mathring{A}^2$/min for the temperature range of 300° to 525°C. The parabolic rate constant changes by a decade in magnitude for every 75°C change in temperature. The bulk tungsten oxidized in the literature had similar magnitudes of parabolic rate constants. Additionally, the parabolic rate constants at higher temperatures, particularly 525°C, varied with time. This

could be the result of two different types of oxide film being formed: a protective scale followed by a porous scale. The activation energy for the parabolic rate constant was found to be approximately 30,000 cal/mole.

The oxide was characterized both physically and optically. The stoichiometry of the oxide film found an outer film of WO_3 and an interface that varies from W to WO_3. Additionally, it was found that the outer WO_3 was uniform, but the interface was a comparatively large region. The electrical resistivity tended to decrease with increasing thickness of oxide. The resistivity was found to vary from approximately 100 Ω-cm to 1000 Ω-cm. The electrical measurements were found to be sensitive to the probe pressure. Additionally, the SNL samples seemed to be more vulnerable to probe pressure than the U of A samples.

The index of refraction was measured using a Ruldoph AutoEL^R-II Ellipsometer. It was found that the index of refraction varied as the thickness varied. The SNL samples in all cases seemed to have a higher index of refraction. The index of refraction was approximately 1.5 for the U of A samples that were oxidized at 300°C, 375°C, and 450°C, whereas the U of A samples oxidized at 525°C had an index of refraction of approximately 2.5. The index of refraction for the SNL samples oxidized at 300°C, 375°C, and 450°C was approximately 2.0. The SNL samples oxidized at 525°C had indexes of refraction that varied between 3.0 and 9.0. Some of the problems encountered in measuring the physical characteristics of the film could be due to the roughness of the surface,

an interface that does not appear to be sharp, and a porous crystaline structure.

The last area that was investigated was the passivation of the thin film tungsten. Both CVD silicon dioxide and LPCVD silicon nitride were used as passivating films. In all cases, the silicon nitride was found to protect the tungsten better. The silicon nitride was used at 450 and 2000Å thicknesses. The samples were then oxidized up to 800°C. The tungsten did not seem to oxidize with the 2000Å film, but did oxidize slightly with the 450Å film. The CVD silicon dioxide did not withstand the temperature above 400°C for longer than one hour.

There are numerous areas that could be further investigated to get a more complete characterization of tungsten oxide. These include:

1. RBS analysis to investigate at what point WO_3 forms.
2. Oxidation of thin film tungsten by other means than just dry oxygen, that is, steam.
3. SEM analysis of the interface.
4. Find the upper limit (temperature) of the silicon nitride passivation film.
5. Defining a selective etch process for tungsten oxide, to enable electrical parameters to be more accurately measured.

APPENDIX A

RUTHERFORD BACKSCATTERING

Rutherford Backscattering (RBS) is used to analyze thin films for properties such as stoichiometry, composition, uniformity, and thickness. Basically, RBS is a technique by which particles are generated by an ion source (helium in this case). The ion energy is then raised by the use of an accelerator, typically a Van de Graff. The ion beam is then focused and filtered to meet system requirements. This beam of ionized particles then bombards the sample of interest causing particles to be reflected back in different directions. The particles that are reflected back by more than 90° are analyzed for reflected energy. The energy comparison between incident and reflected particles is used in the analysis of the properties of interest. Figure 23 is a block diagram of a typical RBS system (Chu, Mayer, and Nicolet 1978).

The RBS system used for the analysis of tungsten oxide is located in the physics department of the University of Arizona. Two beam energies were used for the samples: 1.892MeV and 3.772MeV depending on the features of the sample that was being investigated. The system consisted of a 1024 multichannel analyzer with a solid state detector with solid angle 0.78 Sr. Figure 24 shows the different parameters used in RBS analysis.

The RBS analysis was done on U of A and SNL samples oxidized at 450°C for both 50 and 90 minutes. Additionally, a sample of thin

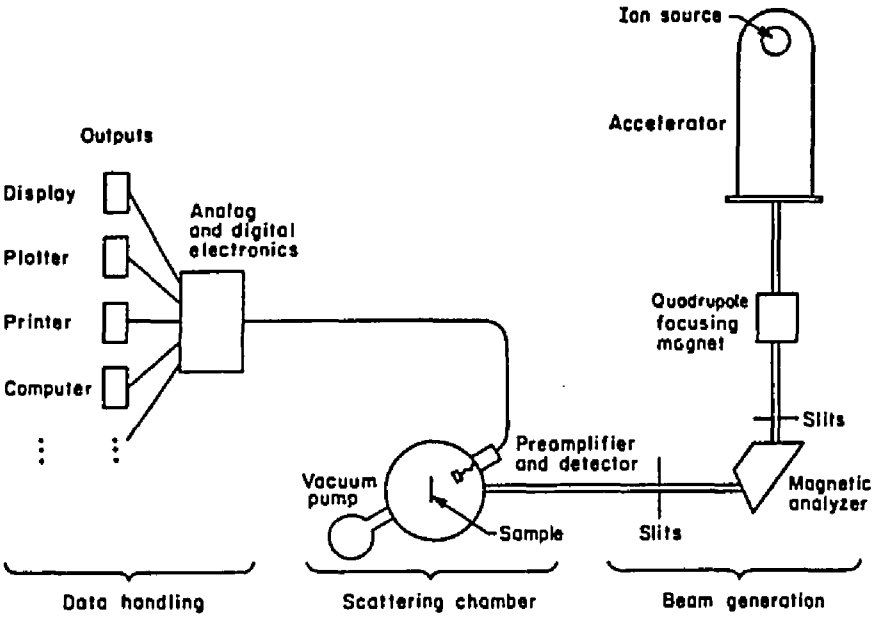

Figure 23. Typical Rutherford Backscattering System.

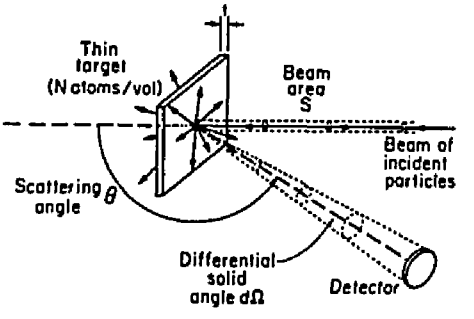

Figure 24. Parameters for RBS Analysis.

film tungsten from both the U of A and SNL were analyzed for background composition. One problem that did arise was that the tungsten samples were too thick for optimizing the RBS spectrum. This in turn caused the tungsten spectrum to mask over the presence of any other elements.

The RBS spectra were analyzed for stoichiometry and thickness. This analysis will be discussed briefly below.

Stoichiometry

The stoichiometry of the films was determined using a comparison of heights between the oxide surface and the pure tungsten surface.

N'_W, N'_O, N_W ≡ The number of atoms per unit volumne for tungsten and oxygen in the oxide and for pure tungsten respectively.

ζ ≡ energy per channel for multichannel analyzer.

t'_W ≡ thickness tungsten oxide layer that causes backscattered energy of +He which scatters from the tungsten to diminish by ζ.

t_W ≡ thickness of layer of pure tungsten that causes backscattered +He's energy to diminish by ζ.

Q ≡ total number of incident particles.

Ω ≡ solid angle subtended by detector at target.

σ_W ≡ scatter cross section of tungsten.

$\theta \equiv$ angle between detector and transmitted beam.

$$h_W = \frac{Q\,\Omega}{\cos\,\theta_1} \cdot \sigma_W \cdot (N_W\,t_W)$$

$$h'_W = \frac{Q\,\Omega}{\cos\,\theta_1} \cdot \sigma_W \cdot (N'_W\,t'_W)$$

Assume Q, Ω, and θ are the same for all runs made on pure tungsten and tungsten oxide. Then,

$$\frac{h_W}{h'_W} = \frac{N_W\,t_W}{N'_W\,t'_W}$$

t_W and t'_W are defined by ($E_{1W} = K_W E_O - \zeta$) which can be interpreted as the thickness of material required to cause an energy shift.

$$\zeta = Z\,N_W\,t_W \text{ and } \zeta = Z\,N'_W\,t'_W + Y\,N'_O\,t'_W$$

Where

$$Z = \left[\frac{K_W\,\varepsilon^W(E_O)}{\cos\,\theta_1} + \frac{\varepsilon^W(K_W\,E_O)}{\cos\,\theta_2} \right]$$

$$Y = \left[\frac{K_W\,\varepsilon^O(E_O)}{\cos\,\theta_1} + \frac{\varepsilon^O(K_W\,E_O)}{\cos\,\theta_2} \right]$$

$$\frac{t_W}{t'_W} = \frac{Z\,N'_W + Y\,N'_O}{Z\,N_W}$$

From data,

$$\frac{h_W}{h'_W} = 1 + \left(\frac{Y}{Z}\right)\frac{N'_O}{N'_W} \qquad \text{from data}$$

$$\frac{N'_O}{N'_W} = \left(\frac{Z}{Y}\right)\left[\frac{h_W}{h'_W} - 1\right]$$

Where K is the kinematic factor defined as the ratio of energy of the particle after collision to the energy of the particle before collision, and ε is the stopping cross section.

Depth Scale of Tungsten Oxide

There are two ways to calculate the tungsten oxide thickness. The first way is an iterative method that uses surface energy analyses to find the density of depth scale profile. The second method, based on energy loss, will be briefly described.

First assume that the oxidized portion of the tungsten is purely WO_3, then the molecular weight is 231.85 and density is 7.16g/cm^3.

$$N_W = 1.86 \times 10^{22} \text{ atom/cm}^3$$

$$N_O = 3\ N_W = 5.58 \times 10^{22} \text{ atom/cm}^3$$

Then using the energy loss method

$$\Delta E = K_W E_o - E_1 = K_W E_o - [K_W(E_o - \Delta E_{in}) - \Delta E_{out})$$

$$\Delta E = K_W\ \Delta E_{in} + \Delta E_{out}$$

$$\Delta E_{in} = \varepsilon^{W}(E_o)(Nt)_W + \varepsilon^{O}(E_o)(Nt)_O$$

$$E_{out} = \frac{\varepsilon^{W}\,(K_W\,E_o)\,(Nt)_W}{\cos\,\theta_2} + \frac{\varepsilon^{O}\,(K_W\,E_o)\,(Nt)_O}{\cos\,\theta_2}$$

Assume a layer of a certain thickness (t) for a film of WO_3 and calculate the corresponding number of target atoms per unit area of both tungsten and oxygen in the tungsten oxide film (N). From this calculate E for the assumed thickness of WO_3 and get eV/Å at a given beam energy. From this depth scale can be calculated in Å/chan.

APPENDIX B

ELLIPSOMETRY

In order to characterize the thickness and index of refraction of a thin film, an ellipsometer can be used. The ellipsometer used was an AutoEL^{R}-II from Rudolph Research located at Sandia National Laboratories. This ellipsometer is a nulling type which incorporates a polarizer (incident beam), analyzer (reflected beam), and compensator. The compensator can be located in either beam; but in this particular instrument, it is in the incident beam. Basically, ellipsometry provides a means of measuring the difference between the known polarization and the angle of incidence of the incident beam and the polarization of the reflected beam from the sample surface. This is accomplished by having the light, which must be monochromatic, pass through the polarizer, the compensator, the sample, and the analyzer.

A particular measurement consists of setting the incident beam and reflected beam at some desired angle of incidence to the sample surface. A stepper motor (in the AutoEL^{R}-II) alternately rotates the polarizer and analyzer until the intensity of the reflected beam is at a minimum compared to the incident beam. From this, two parameters are found--Δ,ψ--which are used to define the physical parameters of interest.

The AutoEL^{R}-II uses a helium neon laser operating at 632.8nm for the monochromatic light source and an angle of incidence to the

normal of the sample surface of 70°. The AutoEL^{R}-II computer programs were set up for specific samples which are used commonly in the semiconductor industry. These samples are typically transparent films on silicon substrates. The ideal sample typically is optically flat, specular, highly reflective, and has a uniform reflective index. Figure 25 shows the typical sample light set up.

The basic equation of ellipsometry is

$$\rho = \tan e_i$$

where

$$\tan \psi = \frac{\tan \psi_r}{\tan \psi_i} \quad ,$$

$$\Delta = \Delta_r = \Delta_i \quad ,$$

$$\tan \psi_r = \frac{|E_p''|}{|E_s''|} \quad ,$$

$$\tan \psi_i = \frac{|E_p|}{|E_s|} \quad ,$$

$$\Delta_i = \varepsilon_p - \varepsilon_s \quad ,$$

and

$$\varepsilon_r = \varepsilon_p'' - \varepsilon_s'' \quad .$$

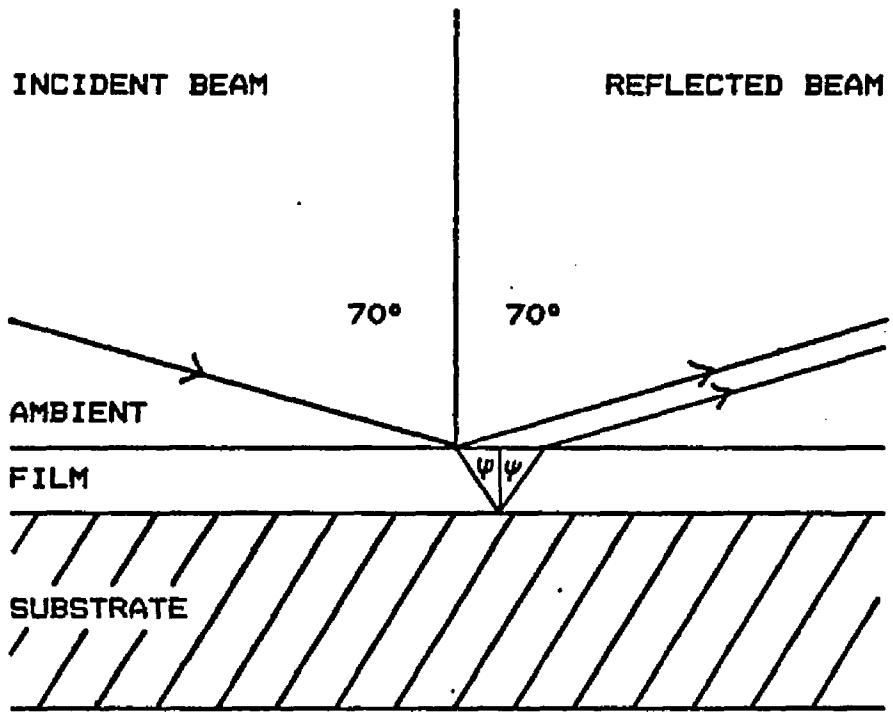

Figure 25. Light Path in Typical Ellipsometer.

$|E_p|$, $|E_s|$ ≡ time independent real amplitudes of incident electric field for parallel and normal component to plane of incidence.

$|E_p''|$, $|E_s''|$ ≡ time independent real amplitude of electric field in reflected beam.

ε_p, ε_s ≡ time independent phases of incident beam for p and s components.

ε_p'', ε_s'' ≡ time independent phases of incident beam for p and s components.

The measurable quantities are Δ and ψ, which are angles. Δ must lie between 0° and 90°, whereas ψ lies between 0° and 360°. Given that Δ and ψ are measured using the ellipsometer for a specific sample and using the basic equation of ellipsometry, the thickness and refractive index can be calculated.

APPENDIX C

OXIDATION PROCESSING PROCEDURE

Listed below are the steps taken to process the bare silicon wafers through tungsten deposition and oxidation. There are seven basic areas of processing. Each major processing step will be described in detail. Photographs of the masks used in the photolithography step are shown in Figures 26 to 28.

I. Thermal Oxidation (U of A Samples Only)

1. Ultra-sonic Clean

   Acetone

   Time: 5 min

2. DI Rinse

   Time: 5 min

3. Piranha Clean

   10:1 H_2SO_4:H_2O_2 (30%)

   Temperature 100°C ± 10°C

   Time: 5 min

4. DI Rinse

   Time: 5 min

5. Oxide Etch

   10:1 H_2O:HF

   Time: 15 sec

6. DI Rinse

Time: 5 min

7. Nitric Acid Clean

   Temperature: 90°C ± 10°C

   Time: 5 min

8. DI Rinse

   Time: 5 min

9. Oxide Etch

   Etchant: 10:1 H_2O:HF

   Time: 15 sec

10. DI Rinse

    Time: 5 min

11. Spin Dry

II. Silicon Dioxide Growth (U of A Samples Only)

Use Bipolar Boron Drive-in Furnace (≈5600Å SiO_2)

1. Dry Oxidation

   By-pass set to 50

   Temperature: 1100°C

   Time: 10 min

   Oxidation Thickness: 400Å

2. Steam Oxidation

   Bubbler set at 60

   Temperature: 1100°C

   Time: 40 min

   Oxidation Thickness: 5200Å

3. Dry Oxidation

By-pass set to 50

Temperature: 1100°C

Time: 10 min

Oxidation Thickness: 100Å

III. Deposition of Tungsten

1. U of A Samples

Cold Wall LPCVD

Deposition Reaction: $WF_6 + 3H_2 \longrightarrow W + 6HF$

2. SNL Samples

Hot Wall Reduced Pressure CVD

Deposition Reactions:

1) $2WF_6 + 3Si \longrightarrow 2W + 3SiF_4$

2) $WF_6 + 3H_2 \longrightarrow W + 6HF$

IV. Photolithography (Resistor Pattern, Contact Windows)

Resist: OMR-183

1. Application

Spin Speed: 4000 rpm

Time: 20 sec

2. Prebake

Temperature: 90°C

Time: 15 min

3. Exposure

Time: 12 sec

4. Development

Time: 20 sec immersion in Xylene

Follow with 5 sec Xylene rinse, N_2 blow dry

5. Postbake

   Temperature: 135°C ± 10°C

   Time: 30 min

6. Tungsten Etch

   Plasma Etch, PDE 1000

   Gas: CF_4

   Etch Rate: 300Å/min

7. Tungsten Wet Etch

   Etchant: 20:1 $K_3Fe(CN)_6$:$H_2NCH_2CH_2NH_2$

   Time: 1 - 2 min (Complete Etch)

8. Photoresist Removal

   A. Strip

      Stripper: No Phenol 922

      Temperature: 100°C ± 5°C

      Time: 10 min

   B. DI Rinse

      Time: 10 min

   C. Sulfuric Acid Clean

      Temperature: 95°C ± 5°C

      Time: 5 min

   D. DI Rinse

      Time: 5 min

V. Tungsten Oxidation

Gas: O_2 at 0.45 liter/min

VI. Metalization

1. Evaporation of Aluminum (2000Å)
2. Photoresist same as IV except:
   A. Aluminum Etch
      Etchant: 40:9:2 H_3PO_4:H_2O:HNO_3
      Temperature: 60°C ± 5°C
      Time: ≈15 - 20 sec
   B. Photoresist Removal
      Stripper: No Phenol 922
      Temperature: 100°C ± 5°C
      Time: 10 min

VII. Passivation

A. Deposition of CVD Silicon Dioxide

Rotox 60

Deposition Rate: 1100Å/min

Etch: 10:1 H_2O:HF

B. Deposition of Silicon Nitride

LPCVD

Deposition Rate: 100Å/min

Etch: H_3PO_4 at 180°C ± 10°C

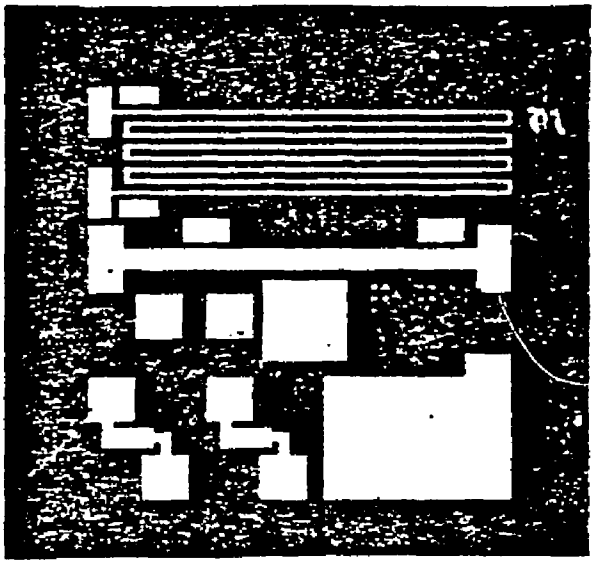

Figure 26. Tungsten Delineation Mask.

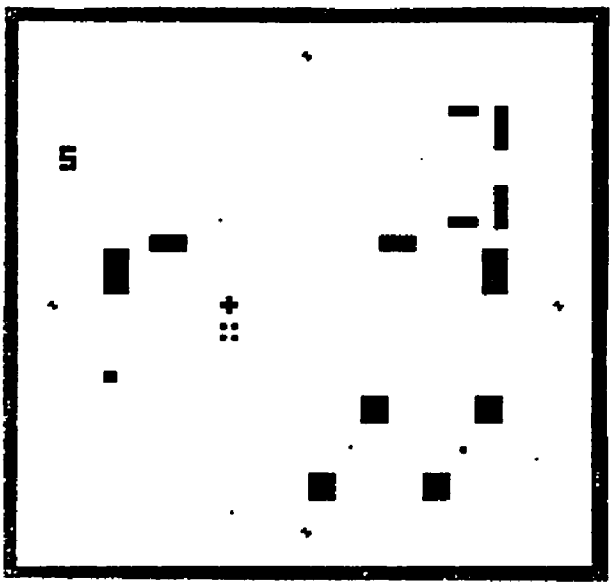

Figure 27. Contact Mask.

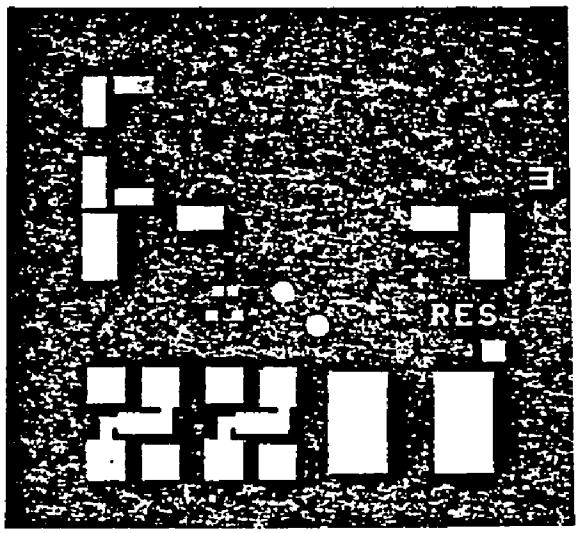

Figure 28. Metalization Mask.

LIST OF REFERENCES

Baur, J.P., D.W. Bridges, and W.M. Fassell, Jr. "High Pressure Oxidation of Metals--Tungsten in Oxygen," J. Electrochem. Soc., Vol. 103, No. 5, 1956.

Chu, Wei-Kan, J.W. Mayer, and M.A. Nicolet. Backscattering Spectrometry. New York: Academic Press, 1978.

Deal, B.E., P.J. Flemming, and P.L. Castro. "Electrical Properties of Vapor-Deposited Silicon Nitride and Silicon Oxide Films on Silicon," J. Electrochem. Soc., Vol. 115, No. 3, 1963.

Fromhold, A.T. Theory of Metal Oxidation, Vol. I and II. New York: North-Holland Publishing Co., 1976.

Gulbransen, E.A. and K.F. Andrews. "Kinetics of the Oxidation of Pure Tungsten from 500°C to 1300°C," J. Electrochem. Soc., Vol. 107, No. 7, 1960.

Harris and Wilson. "Survey of Semiconductor Electrodes," Annual Review of Material Science, Vol. 8, 1978.

Hass, G. and R.E. Thun. Physics of Thin Films, Vol. 5. New York: Academic Press, 1969.

Heavens, O.S. Optical Properties of Thin Solid Films. New York: Dover Publication, Inc., 1965.

Jepson, W.B. and D.W. Alymore. "The Formation of Porous Oxides on Metals," J. Electrochem. Soc., Vol. 108, No. 10, 1961.

Kellett, E.A. and S.E. Rogers. "The Structure of Oxide Layers on Tungsten," J. Electrochem. Soc., Vol. 110, No. 6, 1963.

Kofstad, Per. High-Temperature Oxidation of Metals. New York: John Wiley and Sons, Inc., 1966.

Leavitt, J. Unpublished notes of Rutherford Backscattering analysis of tungsten samples, 1984.

Quarrell, A.G., ed. Niobium, Tantalum, Molybdenum, and Tungsten. New York: Elsevier Publishing Co., 1961.

Rudolph Research. AutoEL^{R}-II Automatic Ellipsometer Instruction Manual, 1980.

Schully, J.C. Fundamentals of Corrosion. New York: Pergamon Press, 1966.

Shaw, J.M. and J.A. Amick. "Vapor Deposited Tungsten for Silicon Devices," Solid State Technology, December 1971.

Webb, W.W., J.T. Norton, and C. Wagner. "Oxidation of Tungsten," J. Electrochem. Soc., Vol. 103, No. 2, 1956.